2. The single track vehicle model

The theory of the linear single track vehicle model with two degrees of freedom is explained in Section 1.3.2. A comparison of this model with experimental data is made using different vehicle tests, e.g. steady state cornering, J-turn, double lane change and random steer. Extensions to include tyre relaxation behaviour and saturation of the tyre forces are also made available.

Some of the material of Sections 1.3.2 and 1.3.3 will be repeated here; more clarified and extended with experimentally found results.

The analysis contains the steady-state and dynamic behaviour using the 'bicycle model' or 'single track vehicle model'. We will deal with the following items.

2.1. The Linear System
2.1.1. Equations of motion
2.1.2. Steady-state cornering
2.1.3. Dynamics
2.1.4. Experimental validation of the vehicle model
2.1.5. Introduction of the relaxation length
2.1.6. Experimental validation
2.2. The Non-Linear System
2.2.1. The handling diagram
2.2.2. Experimental validation

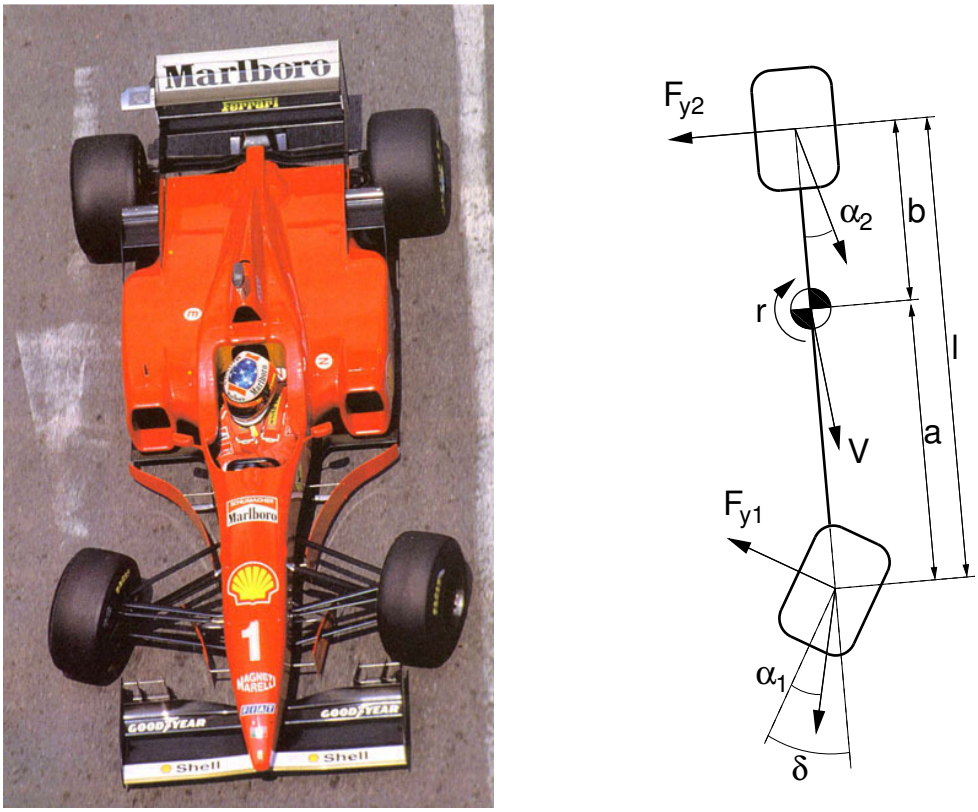

Figure 2.1. Left and right wheels collapsed into a single wheel.

2.1. The Linear System

2.1.1. Equations of motion

assumptions:

- left, right tyre and axle characteristics can be lumped into a single, equivalent "tyre"
- no body roll
- centre point steering
- constant forward velocity u ($\approx V$)
- no aerodynamic forces
- no slopes, level road surface

The steering angle of the front wheel is δ.

The vehicle motion has two degrees of freedom with variables:

- lateral velocity v
- yaw velocity r

We have the following system parameters:
vehicle mass: m
vehicle yaw moment of inertia: I
distances to C.G.: a and b
wheelbase: $l=a+b$

We assume:
small angles δ, α_1, α_2
So that for small x
$\sin(x)= x$ and $\cos(x)= 1$

Note: all equations in this section 2.1 refer to *linear* vehicle behaviour.

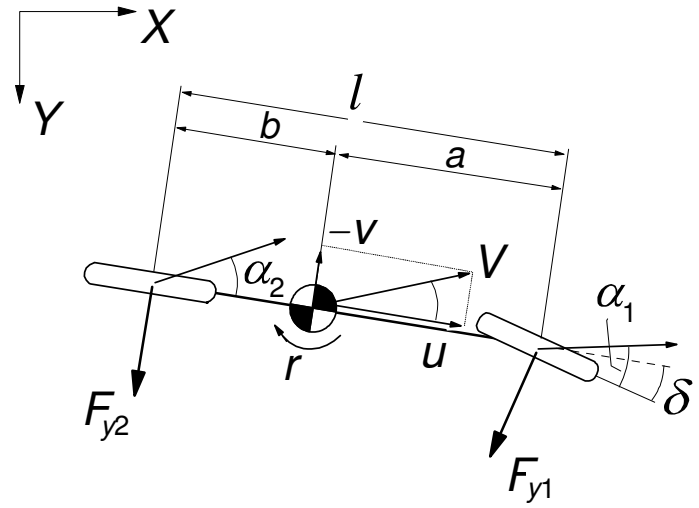

Figure 2.2. The bicycle model.

The equations of motion (cf. Eqs. 1.42a,b) read:

$$\begin{aligned} m(\dot{v} + ur) &= F_{y1} + F_{y2} \\ I\dot{r} &= aF_{y1} - bF_{y2} \end{aligned} \tag{2.1}$$

For the tyre side slip angles we have the relations:

$$\alpha_1 = \delta - \frac{1}{u}(v + ar) \quad , \qquad \alpha_2 = -\frac{1}{u}(v - br) \tag{2.2}$$

The assumed linear cornering characteristic are:

$$F_{y1} = C_1\alpha_1 \quad \text{and} \quad F_{y2} = C_2\alpha_2 \tag{2.4}$$

with C_1 and C_2 the cornering stiffnesses (units: N/rad or, if mentioned: N/deg).
For the vehicle side slip angle we have:

$$\beta = -\frac{v}{u} \tag{2.5}$$

After substitution we get the equations of motion:

$$\begin{aligned} m\dot{v} + \frac{1}{u}(C_1 + C_2)v + \left\{mu + \frac{1}{u}(aC_1 - bC_2)\right\}r &= C_1\delta \\ I\dot{r} + \frac{1}{u}(a^2C_1 - b^2C_2)r + \frac{1}{u}(aC_1 - bC_2)v &= aC_1\delta \end{aligned} \tag{2.6}$$

and after elimination of v:

$$\begin{aligned} &Imu\ddot{r} + \{I(C_1 + C_2) + m(a^2C_1 + b^2C_2)\}\dot{r} + \\ &\frac{1}{u}\{C_1C_2l^2 - mu^2(aC_1 - bC_2)\}r = muaC_1\dot{\delta} + C_1C_2l\delta \end{aligned} \tag{2.7}$$

The equivalent system reads:

$$M\ddot{r} + D\dot{r} + Kr = D_1\dot{\delta} + K_1\delta \tag{2.8}$$

with (cf. Figure 2.3)

$$D = D_1 + D_2\,, \quad K = K_1 + K_2 \tag{2.9}$$

note: r represents the yaw velocity, K may become negative!

We have the expressions

$$\begin{aligned} M &= Imu \\ D &= I(C_1 + C_2) + m(a^2C_1 + b^2C_2) \\ K &= \frac{1}{u}\{C_1C_2l^2 - mu^2(aC_1 - bC_2)\} \\ D_1 &= muaC_1 \\ D_2 &= D - D_1 \\ K_1 &= C_1C_2l \\ K_2 &= K - K_1 \end{aligned} \tag{2.10}$$

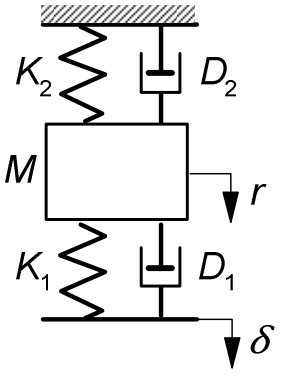

Figure 2.3.
Equivalent system.

2.1.1. Steady-state cornering

- vehicle drives in a circle with fixed radius R
- constant steering angle δ

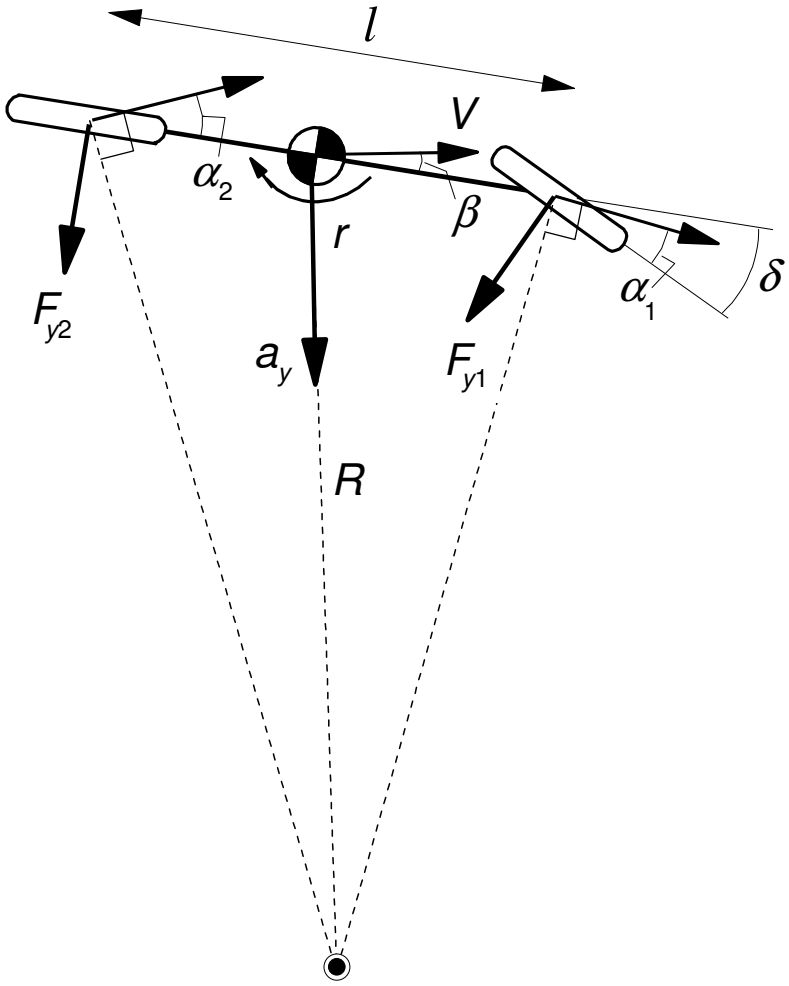

Figure 2.4. Configuration at stead-state cornering.

At steady-state cornering we have:

$$\ddot{r} = \dot{r} = \dot{\delta} = 0 \tag{2.11}$$

The differential equation (2.7) reduces to:

$$\frac{1}{u}\{C_1 C_2 l^2 - mu^2(aC_1 - bC_2)\}r = C_1 C_2 l\delta \tag{2.12}$$

Furthermore:

$$\frac{1}{R} = \frac{r}{V} \approx \frac{r}{u} \qquad \text{(assumption that } \beta \text{ is small)} \tag{2.13}$$

The required steering angle for steady-state driving of a circle with radius *R* becomes:

$$\delta = \frac{1}{R}\left(l - mV^2 \frac{aC_1 - bC_2}{lC_1 C_2}\right) \tag{2.14}$$

or

$$\delta = \frac{l}{R} - \frac{mV^2}{Rl}\left(\frac{a}{C_2} - \frac{b}{C_1}\right) \tag{2.15}$$

1 2

The required steering angle has two contributions:

1. "kinematic" part (ackerman steer)
2. speed (or lateral acceleration) dependent part

With the lateral acceleration

$$a_y = Vr = \frac{V^2}{R} \tag{2.16}$$

we get:

$$\delta = \frac{l}{R} + \frac{a_y}{g}\left\{\frac{mg}{l}\left(\frac{b}{C_1} - \frac{a}{C_2}\right)\right\} = \frac{l}{R} + \frac{a_y}{g}\eta \tag{2.17}$$

We have now introduced the
understeer coefficient or understeer gradient η

$$\eta = \frac{mg}{l}\left(\frac{b}{C_1} - \frac{a}{C_2}\right) \tag{2.18}$$

Other ways of expressing η are:

- using vertical equilibrium:

$$F_{z1,static} = \frac{b}{l}mg \qquad \text{and} \qquad F_{z2,static} = \frac{a}{l}mg \tag{2.19}$$

which leads to

$$\eta = \frac{F_{z1,static}}{C_1} - \frac{F_{z2,static}}{C_2} \tag{2.20}$$

- using expressions (2.2) for the slip angles α_1 and α_2 or geometry (Figure 2.4) we find:

$$\frac{l}{R} = \delta - (\alpha_1 - \alpha_2) \tag{2.21}$$

With (2.17) we have for the difference of the slip angles:

$$\alpha_1 - \alpha_2 = \frac{a_y}{g}\eta \tag{2.22}$$

The steer angle at steady-state cornering becomes now:

$$\delta = \frac{l}{R} + \frac{a_y}{g}\eta \tag{2.23}$$

or

$$\delta = \frac{l}{R}\left(1 + \frac{\eta}{gl}V^2\right) \tag{2.24}$$

Regarding (2.22) the meaning of the understeer coefficient η may be given as follows:

- $\eta = 0$ "neutral steer" ($\alpha_1 = \alpha_2$)
- $\eta > 0$ "understeer" ($\alpha_1 > \alpha_2$)
- $\eta < 0$ "oversteer" ($\alpha_1 < \alpha_2$)

Maintaining a constant radius R while increasing the forward speed V, the steering angle δ:

- can *remain the same* for a neutral vehicle
- has to *increase* for an understeered vehicle
- has to *decrease* for an oversteered vehicle

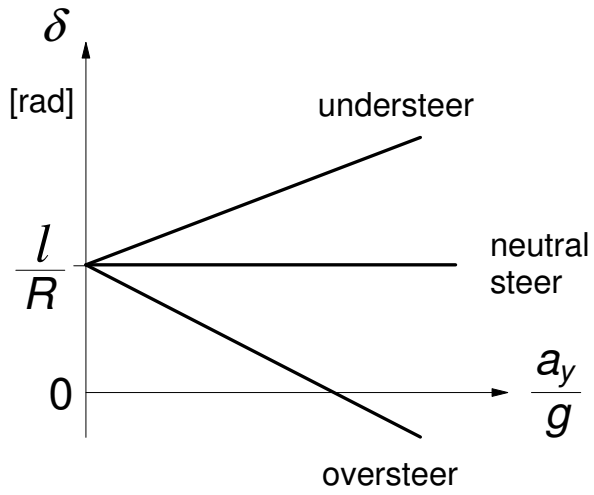

Figure 2.5. Steer angle vs non-dimensional lateral acceleration for the cases understeer, neutral steer and oversteer. The lines show a slope equal to η, cf. Eq.(2.23).

An oversteered vehicle has a critical speed V_{crit} where the required steer angle δ equals zero. We have:

$$V_{crit} = \sqrt{\frac{gl}{-\eta}} \tag{2.25}$$

Beyond this velocity the system is unstable. In the equivalent system the stiffness K will then become negative.
We may also define for an understeered vehicle the characteristic velocity V_{char}.

$$V_{char} = \sqrt{\frac{gl}{\eta}} \tag{2.26}$$

At V=V_{char} twice the steering input is required to maintain the path curvature that holds at very low speeds. At this velocity the steady-state yaw velocity gain reaches its maximum.

The vehicle side slip angle

The vehicle side slip angle β is

$$\beta = -\frac{v}{u} \approx -\frac{v}{V} \tag{2.27}$$

with

$$\alpha_2 = -\frac{1}{u}(v - br) = \beta + \frac{br}{u} \tag{2.28}$$

We find at circular driving with fixed radius R ($=u/r$) :

$$\alpha_2 = \beta + \frac{b}{R} \tag{2.29}$$

and

$$\beta = -\frac{b}{R} + \alpha_2 \tag{2.30}$$

furthermore we may write:

$$\alpha_2 = \frac{F_{y2}}{C_2} = \frac{1}{C_2}\,\frac{mV^2}{R}\,\frac{a}{l} \tag{2.31}$$

Thus with (2.29):

$$\beta = -\frac{b}{R} + \frac{am}{C_2 l}\,\frac{V^2}{R} \tag{2.32}$$

Note: at increasing forward speed V the vehicle side slip angle β changes sign at a certain (low) value of the speed, where β=0. At positive path curvature $1/R$, the angle changes, starting from $-b/R$ at zero speed, to exceed at increasing speed the value zero, thereby becoming positive.

Example: Neutral vehicle (δ fixed), at increasing values of speed V.

1. Speed is assumed to be very low:

$$\alpha_1 \approx 0, \qquad \alpha_2 \approx 0, \qquad \beta \approx -\frac{b}{R}, \qquad \delta \approx \frac{l}{R} \tag{2.33}$$

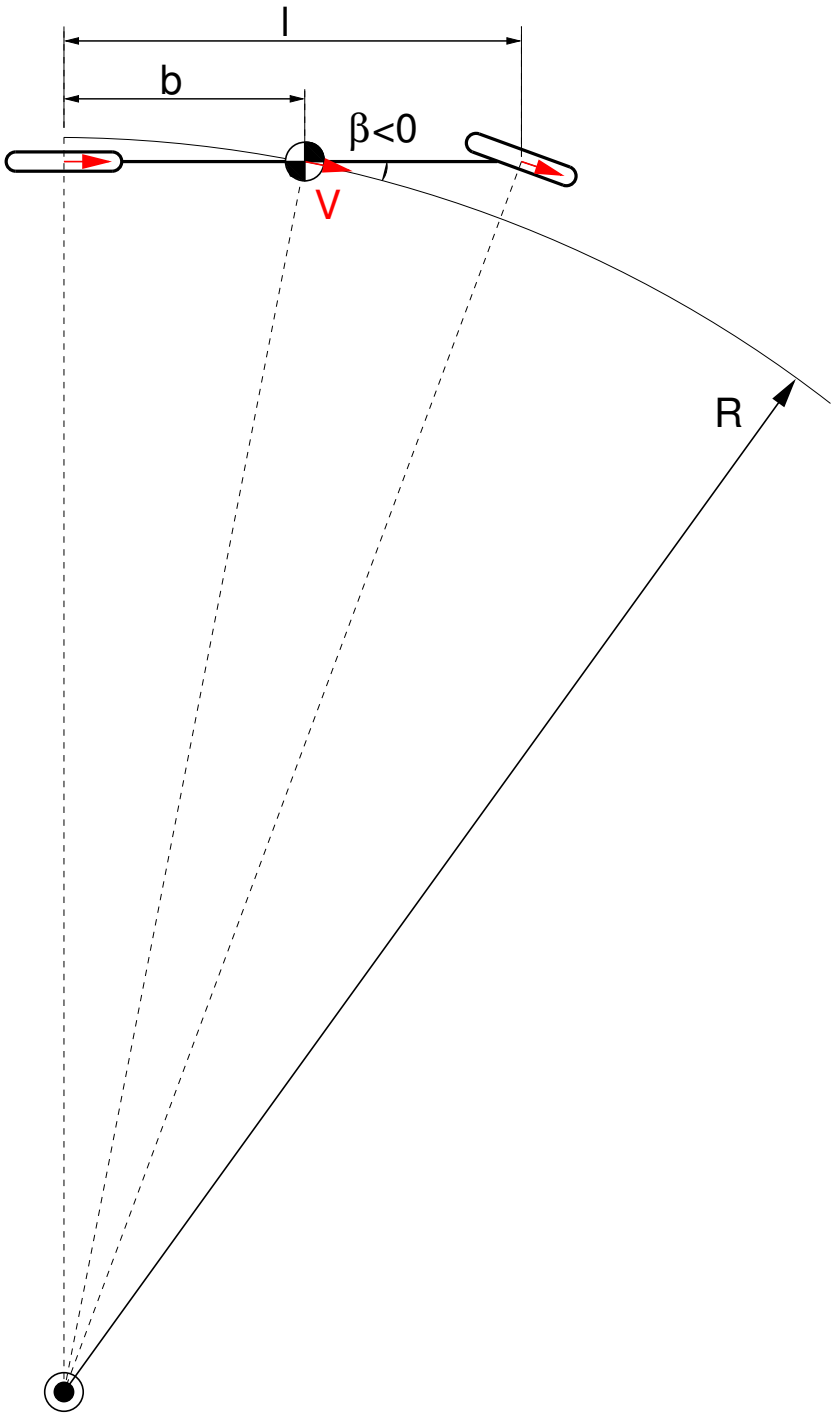

Figure 2.6. Steady-state cornering at speed very low.

2. Cornering at the value of speed V where β becomes equal to zero.

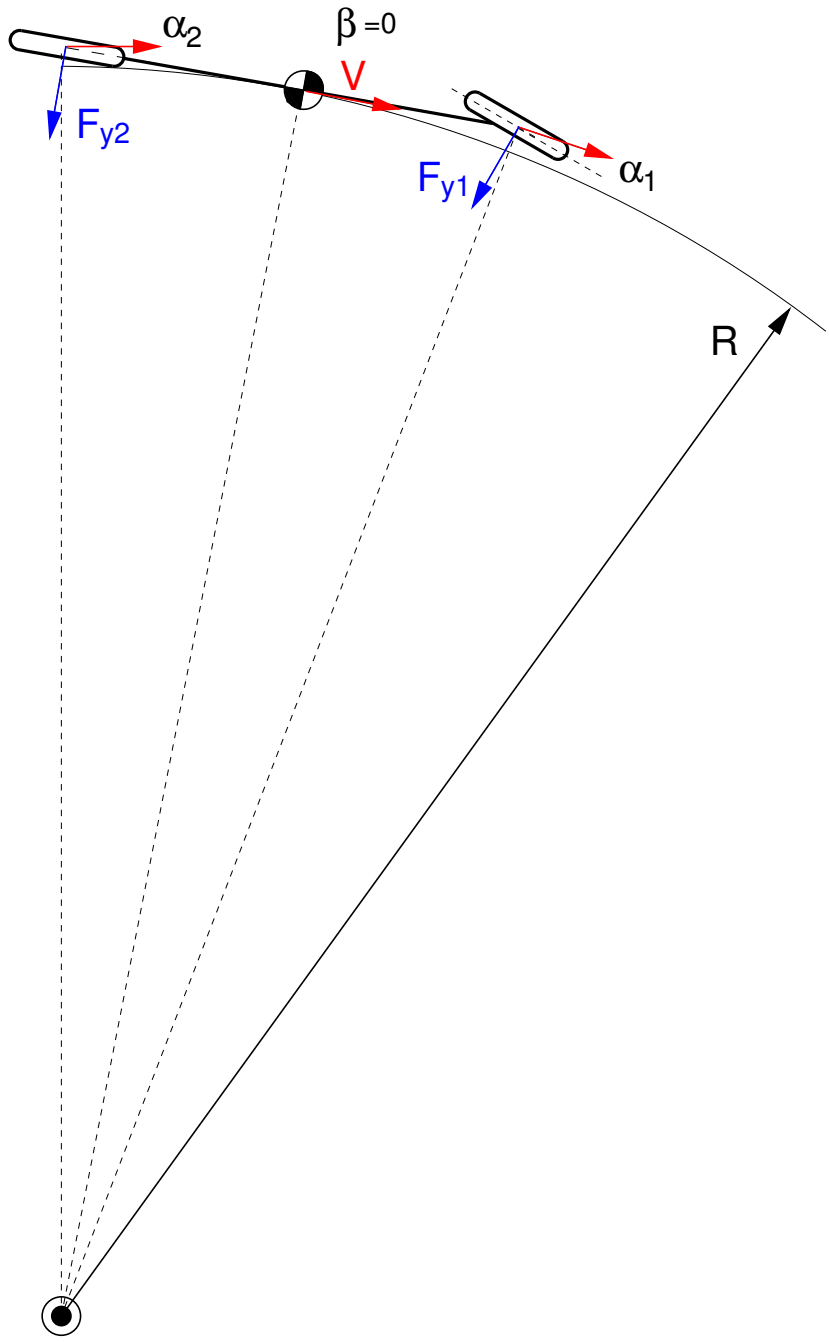

Figure 2.7. Steady-state cornering at value of speed where the vehicle side slip angle becomes equal to zero.

3. Increasing the speed V further: β gets the same sign as the α's .

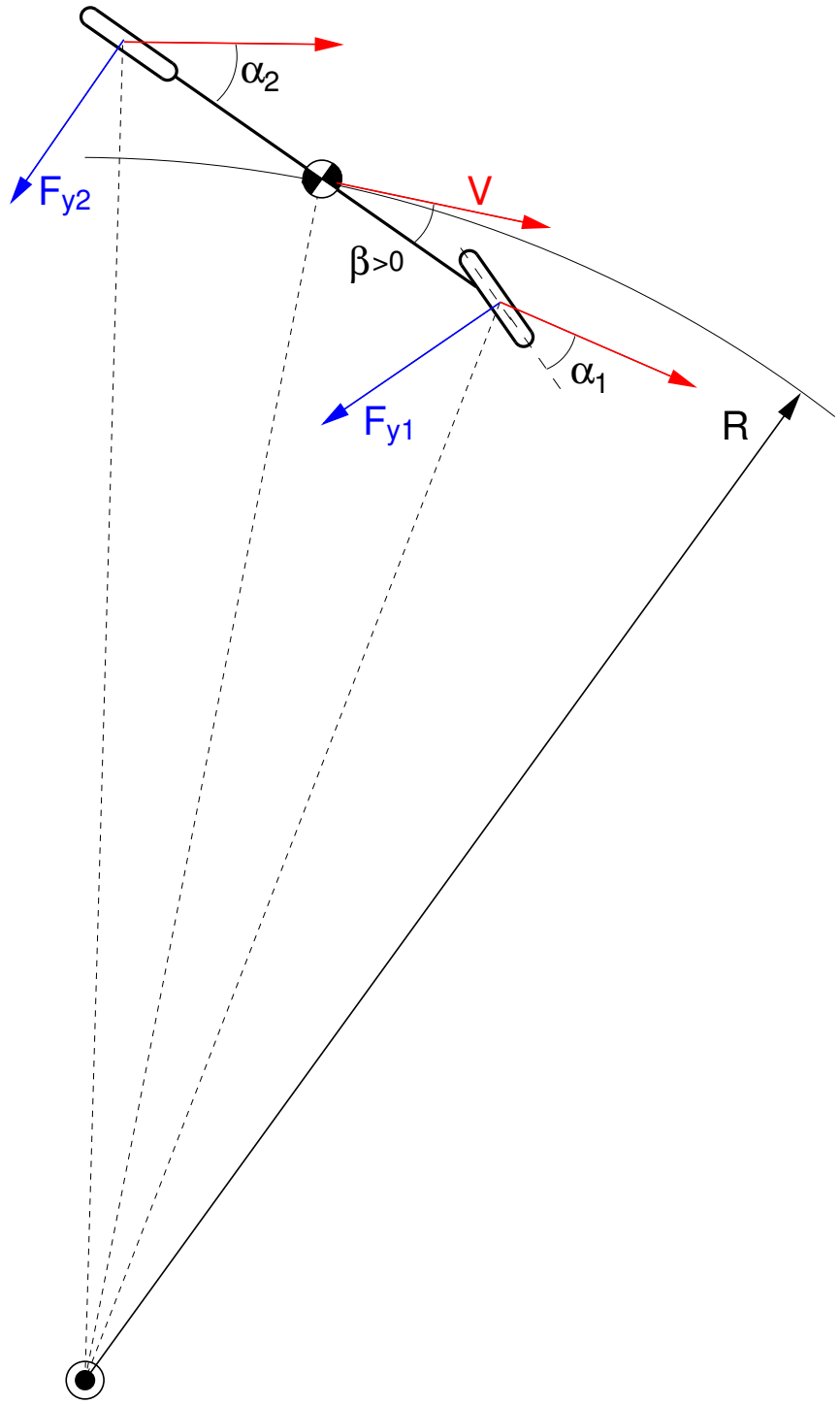

Figure 2.8. Steady-state cornering at higher speed where the signs of the slip angles are the same.

Summarising…

The side force equilibrium

If we increase the forward velocity V and want to maintain the same corner radius R, the lateral tyre forces F_{y1} and F_{y2} have to increase and therefore also the side slip angles will increase.

If we don't change the steering angle δ of a neutral steer vehicle and increase the speed, the front tyre will show the same increase in side slip angle as the rear tyre, thereby keeping the curvature $1/R$ unchanged.

The yaw moment equilibrium

If the increase in lateral force for the front tyre is too small, the driver has to increase the steering angle δ to maintain moment equilibrium:

The vehicle shows understeer

If the increase in lateral force for the front tyre is too big, the driver has to decrease the steering angle δ to maintain moment equilibrium:

The vehicle shows oversteer

If no additional steering action is required:

The vehicle shows neutral steer

An almost trivial example:

Suppose $a = b$

…then the vehicle has neutral steer if the front and rear tyre cornering stiffnesses are equal: $C_1 = C_2$.

…then the vehicle has oversteer if the front cornering stiffness is higher than the rear tyre cornering stiffness: $C_1 > C_2$

…then the vehicle has understeer if the front cornering stiffness is lower than the rear tyre cornering stiffness: $C_1 < C_2$

2.1.3. Dynamics

From previous equations we find for the system stiffness K, cf.Eqs.(2.10), (2.18) in terms of η:

$$K = \frac{1}{u} C_1 C_2 l^2 \left(1 + u^2 \frac{\eta}{gl}\right) \tag{2.34}$$

The stiffness K can become negative if $\eta < 0$ (oversteer). If the speed u exceeds the critical speed, the system becomes unstable. The quantities D and M are always positive, cf. Eqs.(2.10).

Eigenvalues

- neutral and oversteer vehicles have real eigenvalues
- oversteer vehicle has a positive real eigenvalue if $u > u_{\text{crit}}$ (2.25) with $\eta < 0$. Consequently, the system becomes unstable in this range of speed.
- understeer vehicle has complex conjugate eigenvalues. The damping ratio ζ decreases with forward velocity.

We may assume $k = \sqrt{I/m} \approx \frac{1}{2} l$ and $C_1 C_2 \approx \frac{1}{4}(C_1 + C_2)^2$ to simplify the expressions. We have:

The undamped natural frequency

$$\begin{aligned} \omega_o^2 = \frac{K}{M} &= \frac{C_1 C_2 l^2}{m^2 k^2 u^2}\left(1 + \frac{\eta}{gl} u^2\right) \\ &\approx \left(\frac{C_1 + C_2}{mu}\right)^2 \left(1 + \frac{\eta}{gl} u^2\right) \end{aligned} \tag{2.35}$$

The damping ratio:

$$\zeta = \frac{D}{2M\omega_o} \approx \frac{1}{\sqrt{1 + \frac{\eta}{gl} u^2}} \tag{2.36}$$

The natural frequency (cf. Figure 2.9):

$$\omega_n^2 = \omega_o^2 (1 - \zeta^2) \approx \left(\frac{C_1 + C_2}{m}\right)^2 \cdot \frac{\eta}{gl} \tag{2.37}$$

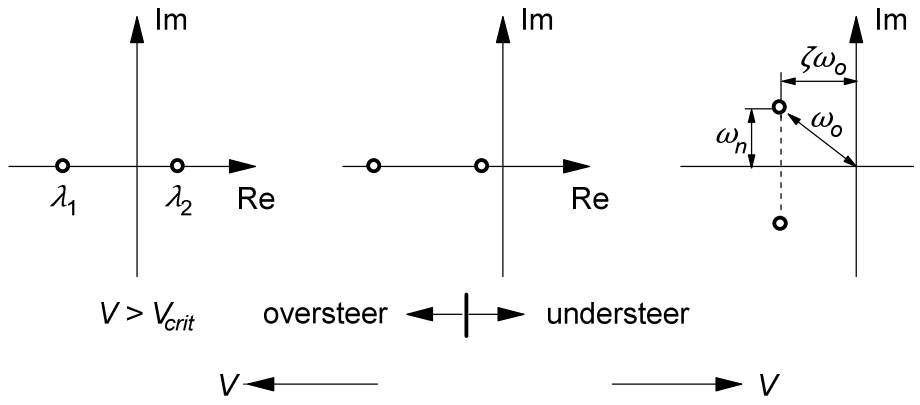

Figure 2.9. Possible eigenvalues for the over and understeered car.

Numerical example

The following parameter values hold:
m=1600 kg, I= 3600 kgm^2,
l= 3 m, a= 1.4 m,
C_1=C_2=60000 N/rad.
$\Rightarrow$ understeer coefficient η = 0.0174 rad

We have complex eigenvalues

$$\lambda = a \pm ib = -\zeta\omega_o \pm i\omega_n \tag{2.38}$$

with

- the frequency in Hz

$$f = \frac{b}{2\pi} \tag{2.39}$$

- the damping ratio in %

$$\zeta = -\frac{a}{|\lambda|} \cdot 100 \tag{2.40}$$

In the diagrams of Figure 2.10 the variation of the natural frequency and of the damping ratio with speed has been presented using the exact expressions for M, D and K given by Eqs.(2.10). It may be noted that for low values of speed the eigenvalues of the understeered car become real and consequently the natural frequency vanishes (also see Figure 2.9).

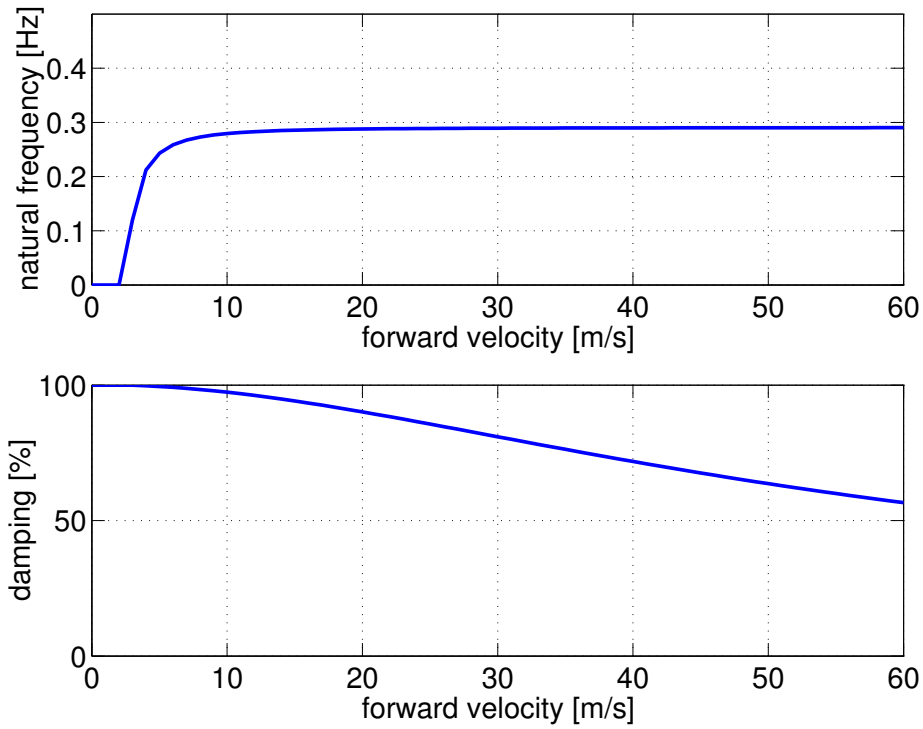

Figure 2.10. Variation of natural frequency and damping ratio with speed.

Response to step change in steer angle

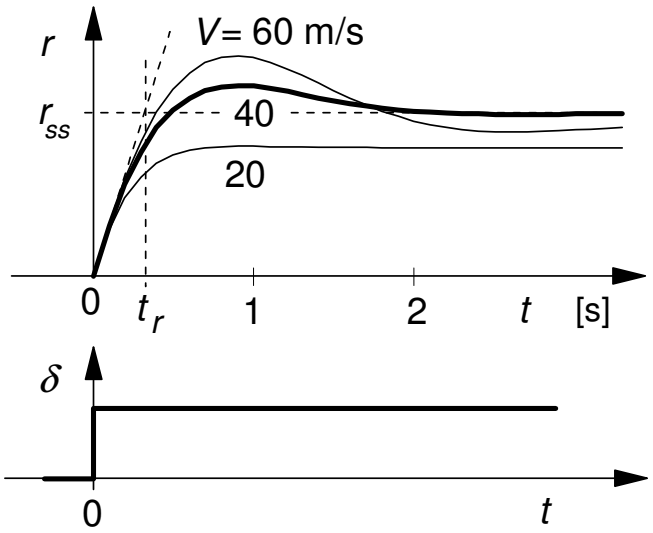

Figure 2.11. Yaw rate response to a step change in steer angle.

In Figure 2.11 the calculated step response has been shown for three different values of speed. The yaw response rise time t_r as indicated in the diagram, can be found from the expression:

$$t_r = \frac{r_{ss}}{\left(\frac{\partial r}{\partial t}\right)_{t=0}} = \frac{IV}{aC_1 l\left(1 + \frac{\eta}{gl}\,V^2\right)} \tag{2.41}$$

In Figure 2.12 the responses of the lateral acceleration a_y, the yaw rate r, the vehicle slip angle β and the wheel slip angles α_1 and α_2 to one degree steer angle change δ has been presented.
Figure 2.13 gives these responses at a speed V=30m/s for the three cases:

- US: understeer
- NS: neutral steer
- OS: oversteer

The magnitude of the δ step has been adapted to approach a yaw rate of 10 deg./s.

Note:

- For an understeered vehicle:
  The response time t_r reaches a maximum at V_{char}.
- The understeered vehicle has a smaller response time t_r compared to an oversteered vehicle.

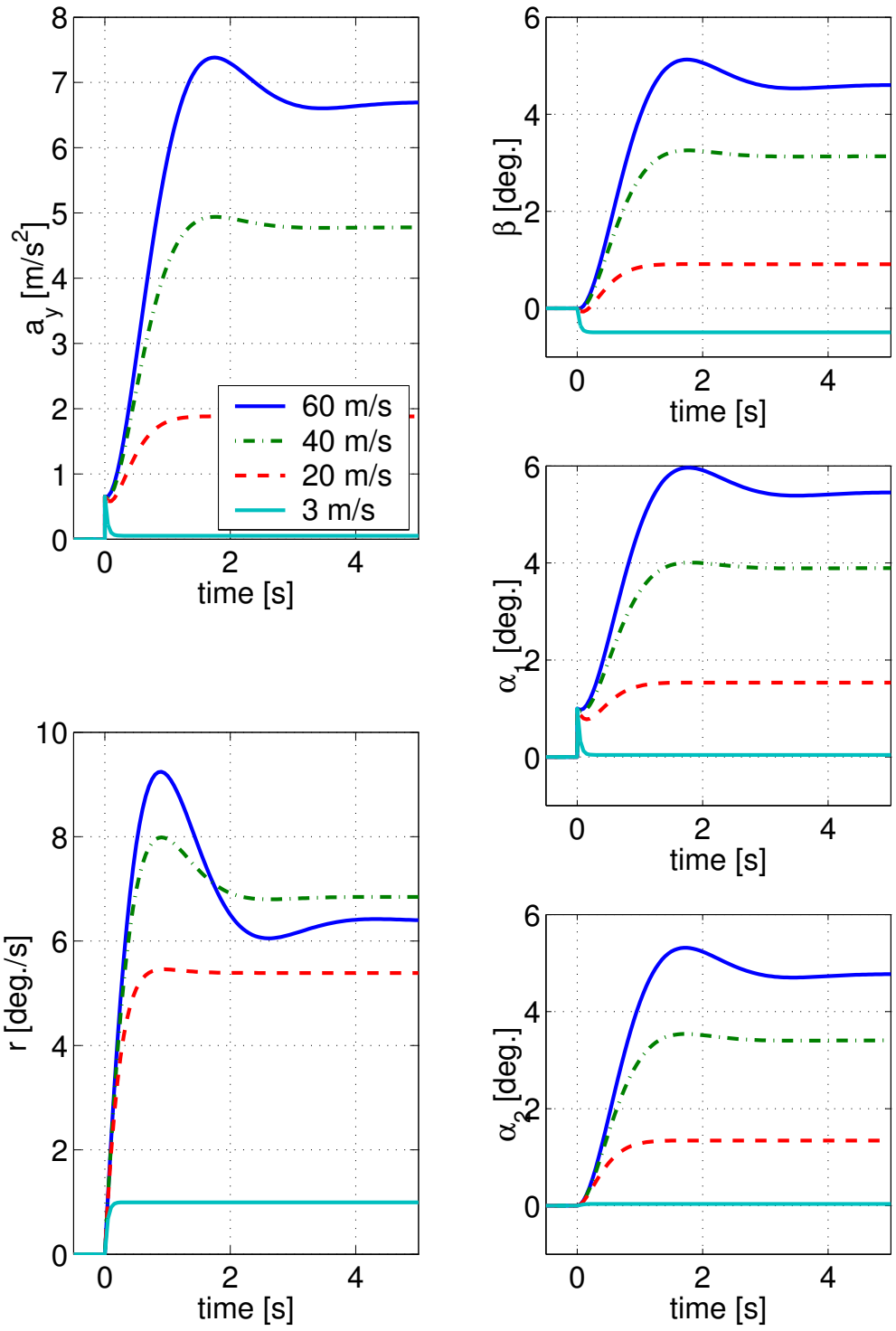

Figure 2.12. Step responses to a step of 1 deg. steer angle at different speeds..

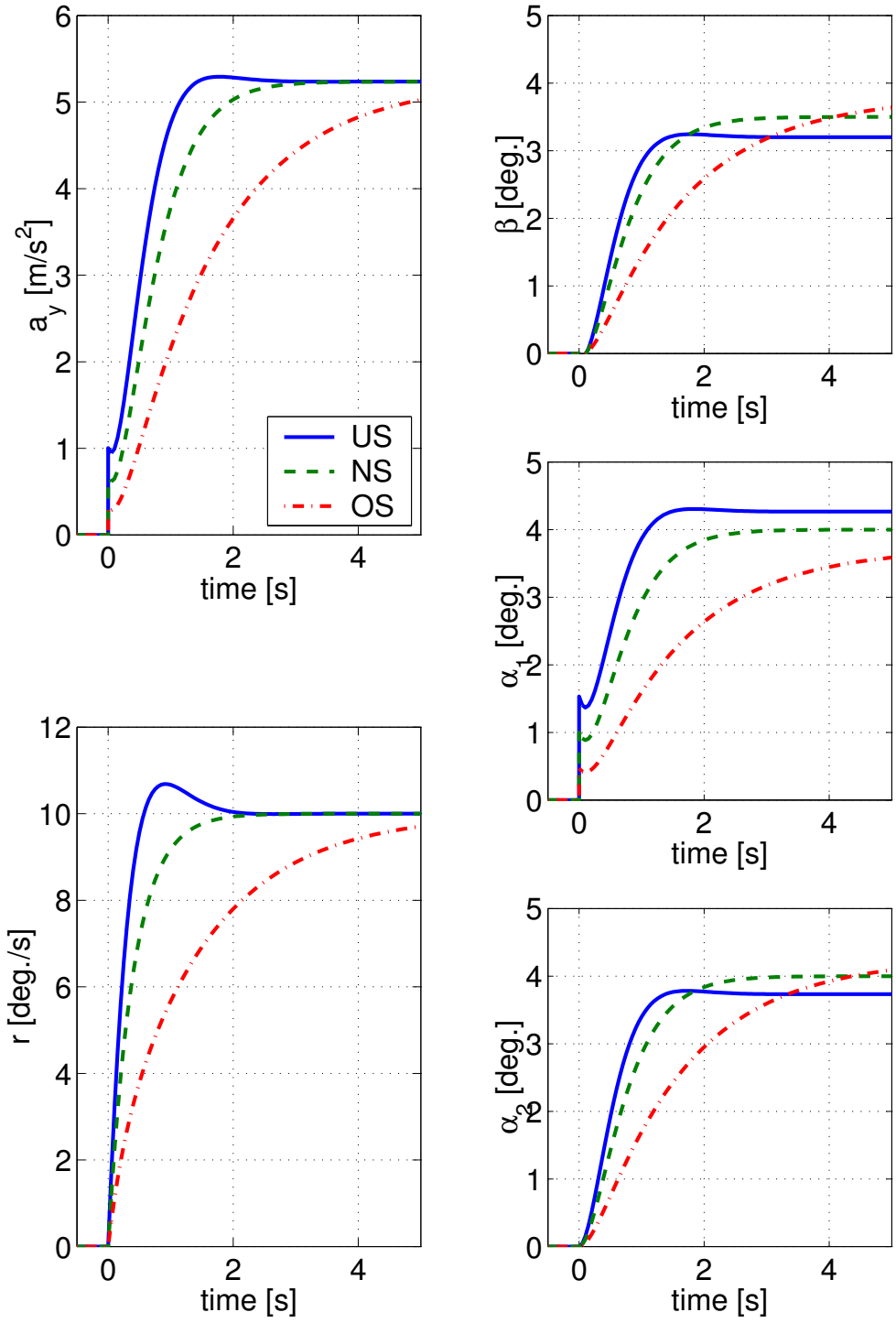

Figure 2.13. Step responses to an adapted step change in steer angle for an understeer (US), a neutral steer (NS) and an oversteer (OS) vehicle.

Frequency response functions with respect to steer angle

In Figures 2.14 and 2.15 the frequency response functions to the steer angle δ have been shown in a logarithmic scale for a_y and r respectively (cf. FIGURE 1.15 of Section 1.3.2 using linear scales).

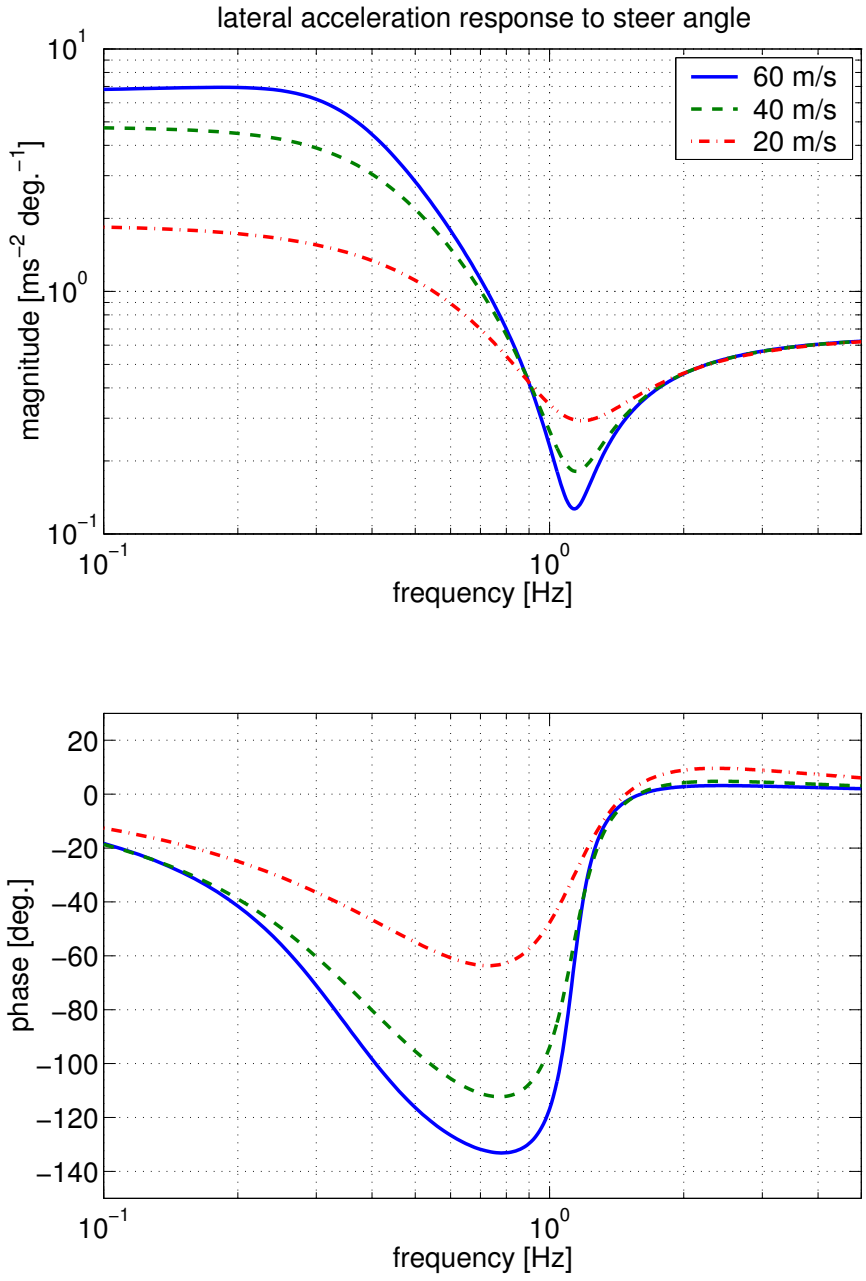

Figure 2.14. Frequency response for lateral acceleration a_y.

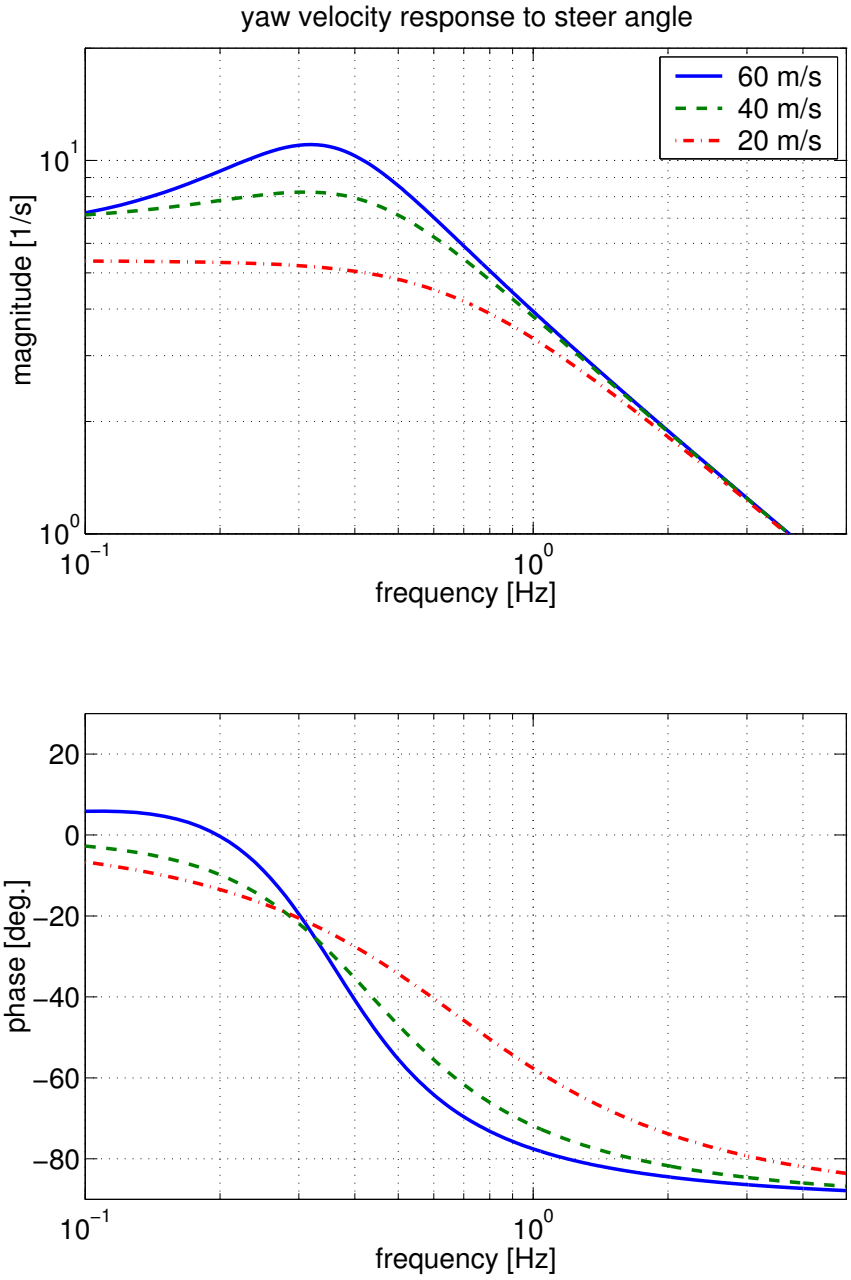

Figure 2.15. Frequency response for the yaw rate r.

2.1.4. Experimental validation of the single track model

Analysis of the cornering and the dynamic response behaviour using the "single track vehicle model".

- Comparison of vehicle model performance with vehicle test results.
- Introducing tyre relaxation effects
- Extension to non-linear behaviour (handling diagram)

The tests have been performed by *TNO Automotive*, Helmond, The Netherlands. We are grateful for their permission to use the test results.

Figure 2.16. Testing at the IDIADA (Spain) proving ground.

Vehicle tests

Instrumented vehicle. Measurement of:

- steer angle, steer torque
- brake pedal force
- forward, lateral and yaw velocity
- longitudinal, lateral acceleration
- roll angle
- travelled distance

Figure 2.17. The TNO instrumented vehicle.

Test track (proving ground)

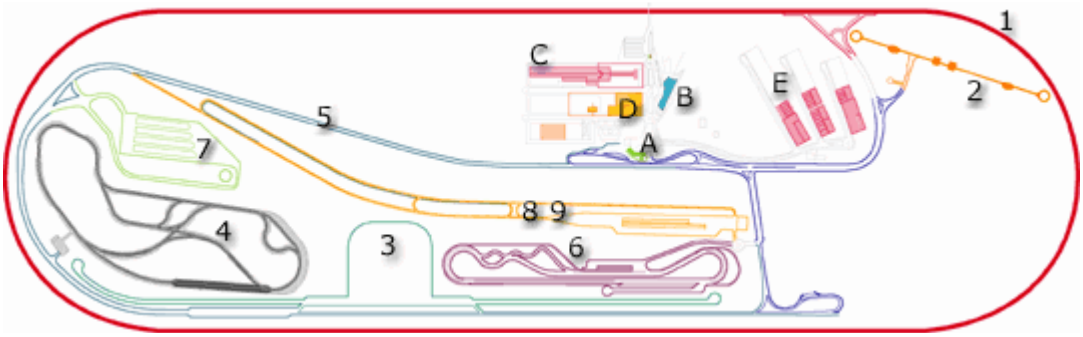

example: IDIADA, Spain

"dynamic platform" (3)

- dimensions 250x250 m
- completely level surface, gradient 0%
- marked circles (range R=10 - 120 m)

Figure 2.18. The IDIADA proving ground.

Steady-state circular test

- fixed radius R (in example shown: 100 m)
- different constant forward velocities V
- steering angle adjusted to maintain radius R
- steady-state conditions

Standardised in ISO 4138
left and right turn

Note:
Data for the left hand turn is mirrored for easy comparison with the right turn (symmetry check)

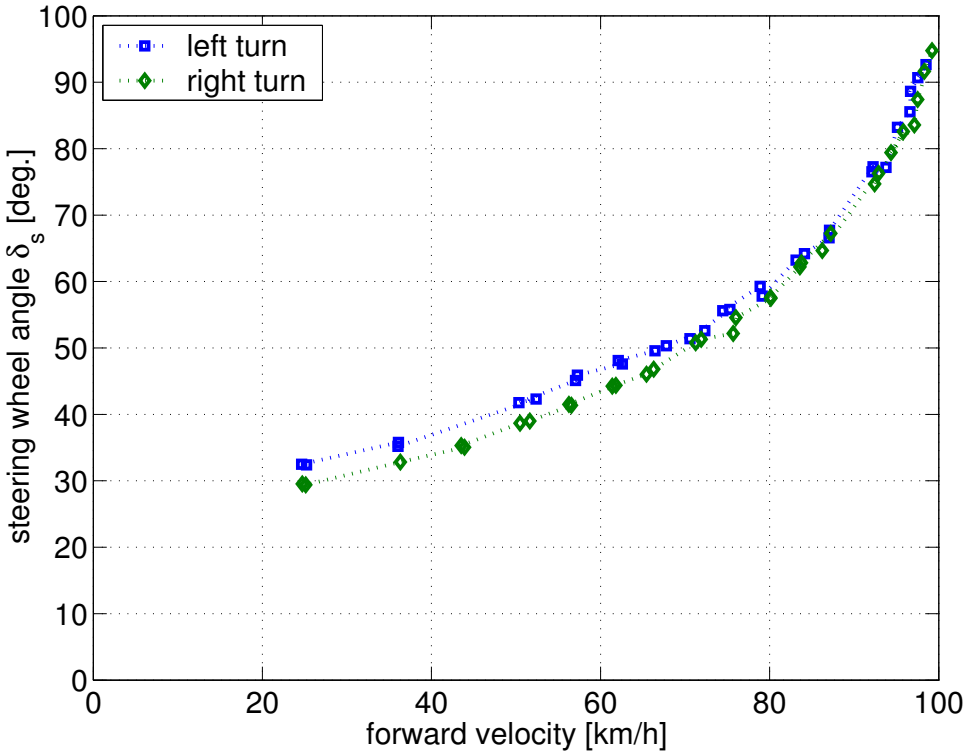

Figure 2.19. Steady-state cornering test at constant radius R=100m.

Checking the resulting radius R

Using the measured quantities:

$$a_y = \frac{V^2}{R} \tag{2.42}$$

$$r = \frac{V}{R} \tag{2.43}$$

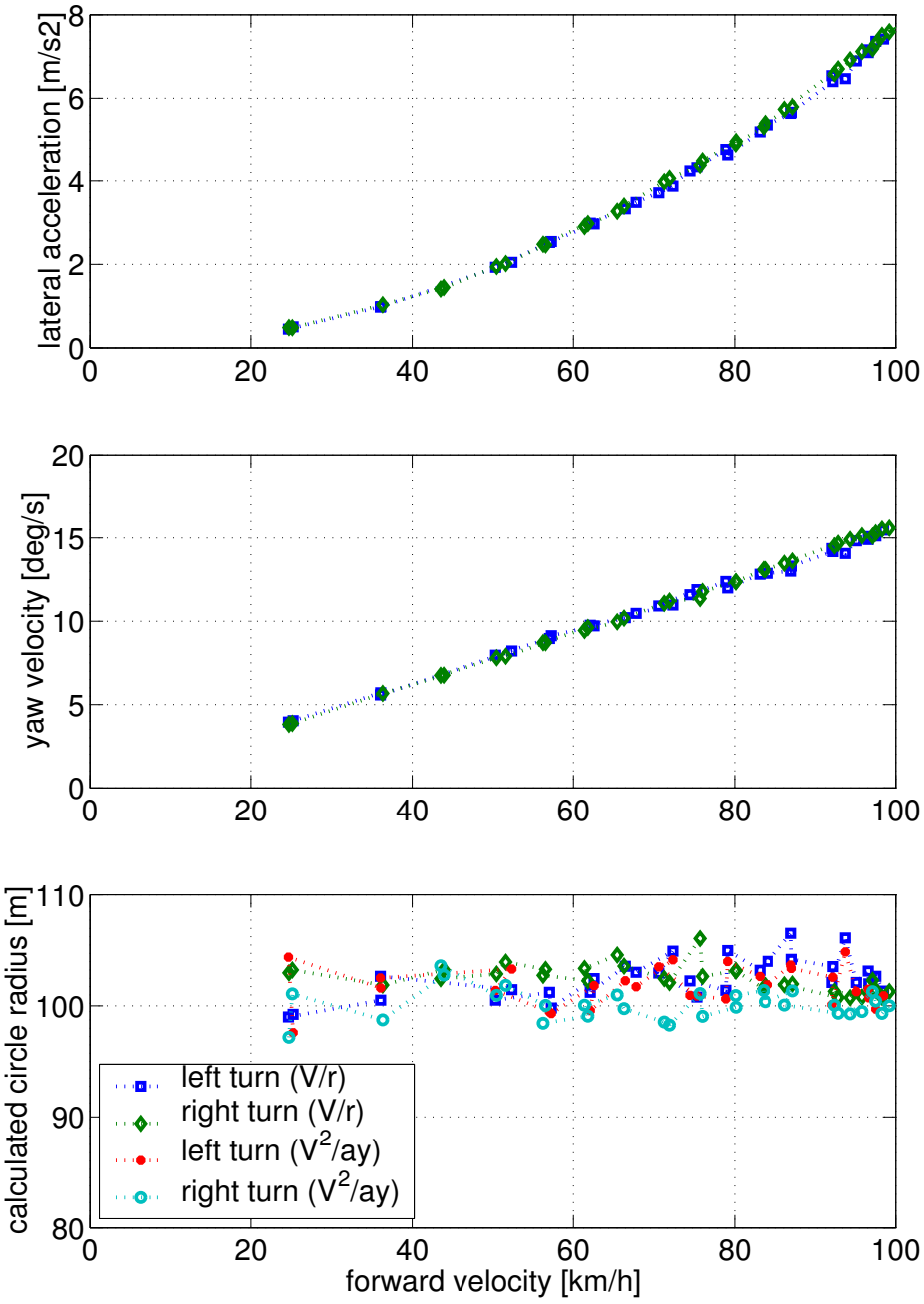

Figure 2.20. Checking the resulting radius R .

Steady-state relationship for steer angle vs lateral acceleration

As a result we obtain the relationship: front wheel steer angle δ vs non-dimensional lateral acceleration a_y/g.

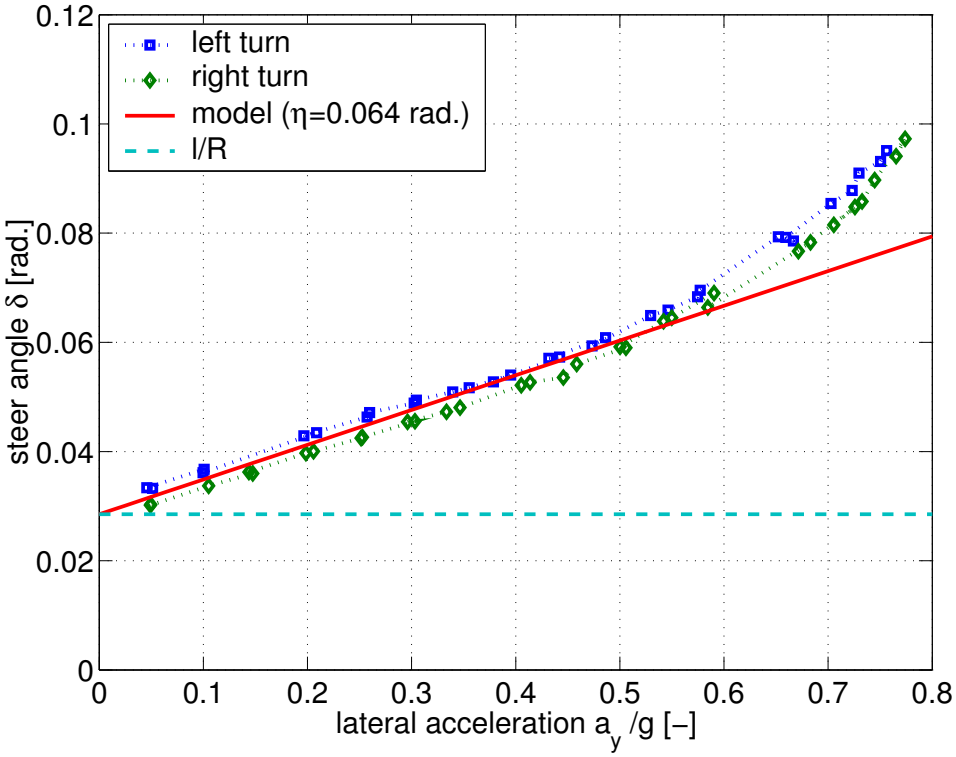

Figure 2.21. Steer angle δ vs non-dimensional lateral acceleration a_y/g at increasing speed and constant radius R.

Conclusions:

- the vehicle obviously shows understeer
- we have linear behaviour up to 0.4 - 0.5 g; differences show up at higher lateral accelerations due to non-linear tyre behaviour

Model parameters:

- based on measurements (e.g. m, l, a, b)
- "tuned" to match tests (e.g. I, C_1, C_2)
- steering ratio

$$i_s = \frac{\delta_{steering\ wheel}}{\delta_{front\ wheel}} \qquad \text{(typically 15 to 20)}$$

Steady state yaw velocity gain

From Eq.(2.24) we can derive the relationship for the yaw rate gain for the linear model:

$$\frac{r}{\delta} = \frac{V/l}{1 + \frac{\eta}{gl}V^2} \tag{2.44}$$

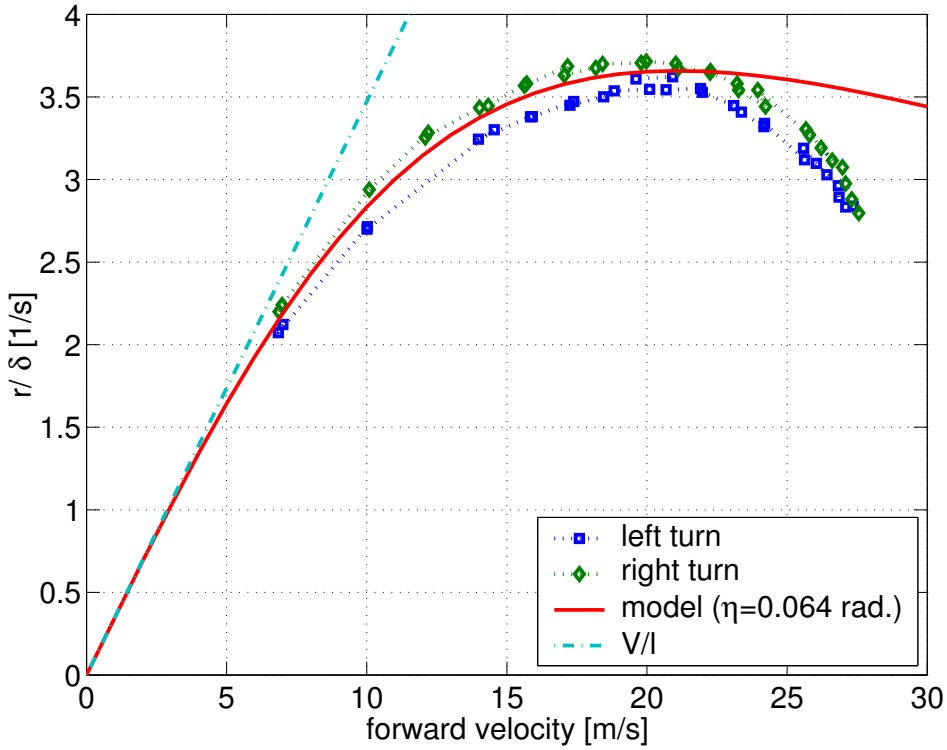

Figure 2.22. Yaw rate response at constant radius and increasing speed.

The diagram confirms that car shows understeer behaviour. We observe that

- $V_{char} \approx 20$ m/s (=72 km/h) (maximum yaw rate response)
- The deviation gets larger for higher forward velocities (in this test: at $V \approx 20$ m/s, where according to Figure 2.20 we have $a_y \approx 4$ m/s^2).

Vehicle side slip angle vs lateral acceleration

From Eq.(2.32) we find a linear relation between β and a_y for the linear vehicle.

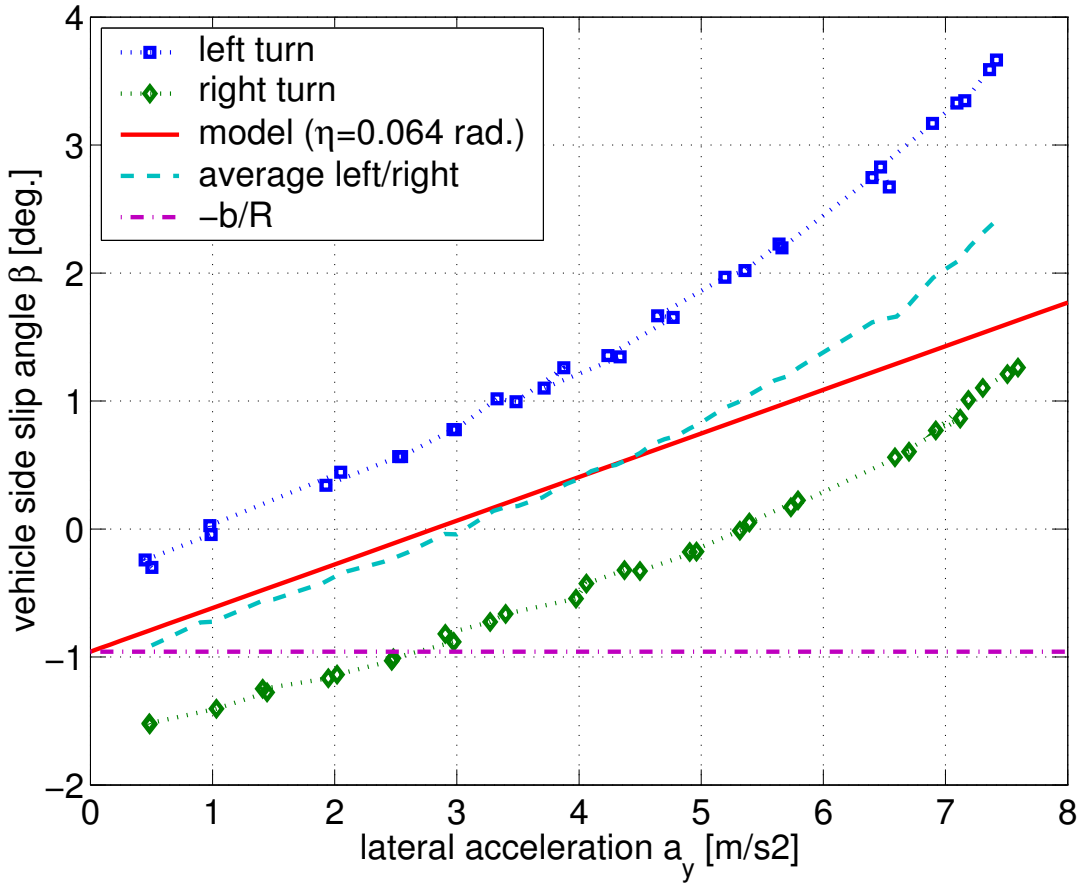

Figure 2.23. The vehicle side slip angle vs lateral acceleration at R=100m.

Note:

- up to 4-5 m/s^2 the response is fairly linear
- the deviation gets larger for higher lateral acceleration levels
- relatively large difference between left and right turn. The cause is not clear (tyre ply-steer?)

Random steering input test

Conditions:

- constant forward velocity
- "pseudo" random steer input using:
  –experienced test driver
  –steering robot
- accelerations within "linear" range (< 4 m/s^2)
- measured in sequences (total time: > 15 min.)

Standardised in ISO 7401 and ISO/TR 8726.

The aim of the test is the determination of transfer functions.
Comparison of the test results with those of the single track model.

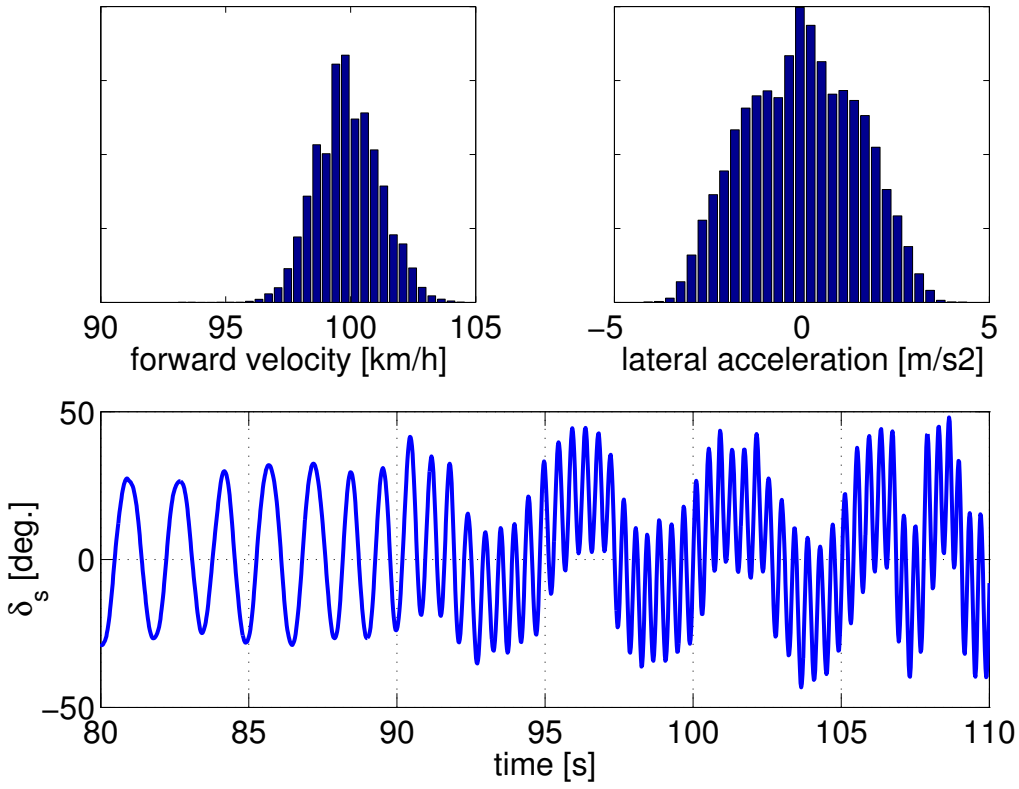

Figure 2.24. Steer angle input in vehicle test on the road.

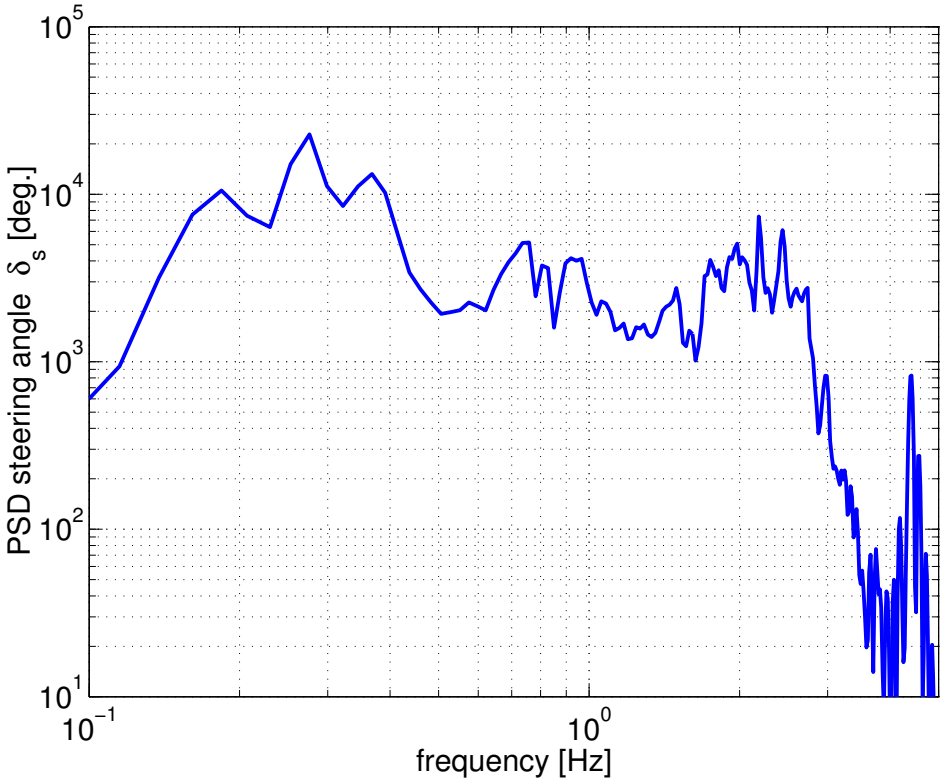

Figure 2.25. Power spectral density of the steering input.

The frequency response functions of the lateral acceleration and of the yaw velocity have been presented in Figures 2.26 and 2.27 both according to the experimental findings and for the model.

Note;

- The vehicle model is still very simple. It does not include e.g. body roll, which is an important source of differences in the lateral acceleration.
- The vehicle model moves at a constant forward velocity of 100 km/h.

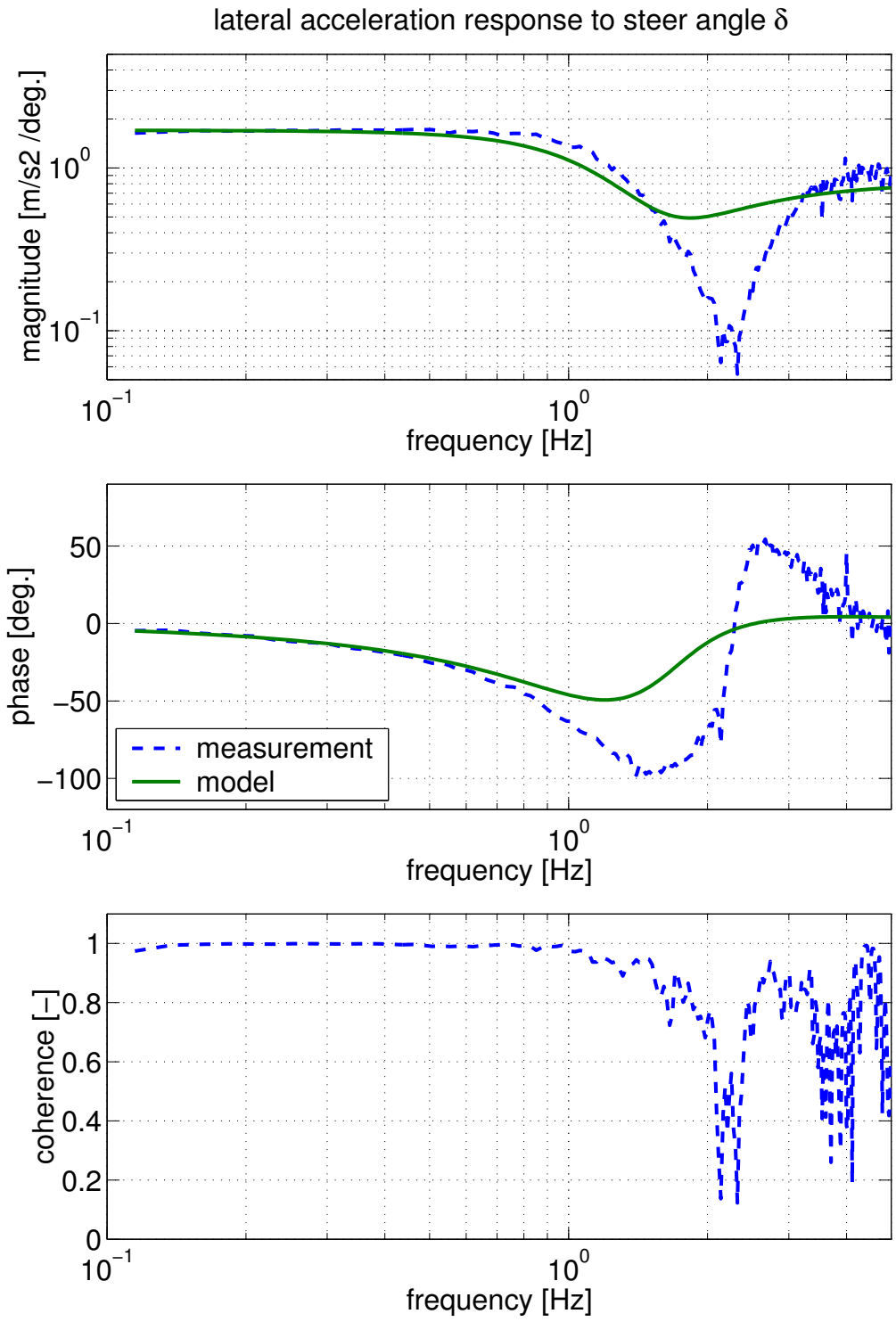

Figure 2.26. The frequency response functions of the lateral acceleration

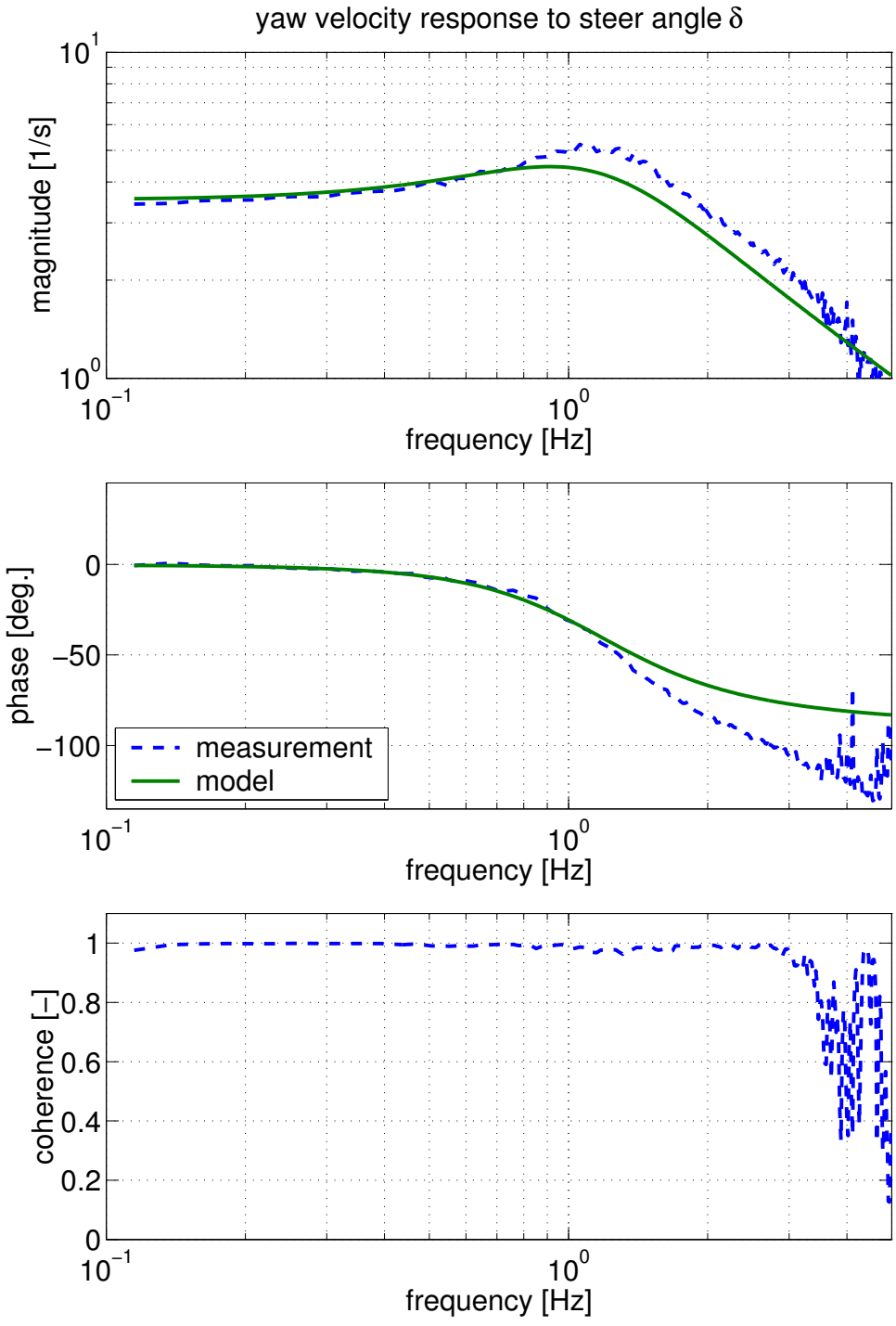

Figure 2.26. The frequency response functions of the yaw velocity.

2.1.5. Introduction of the tyre relaxation length

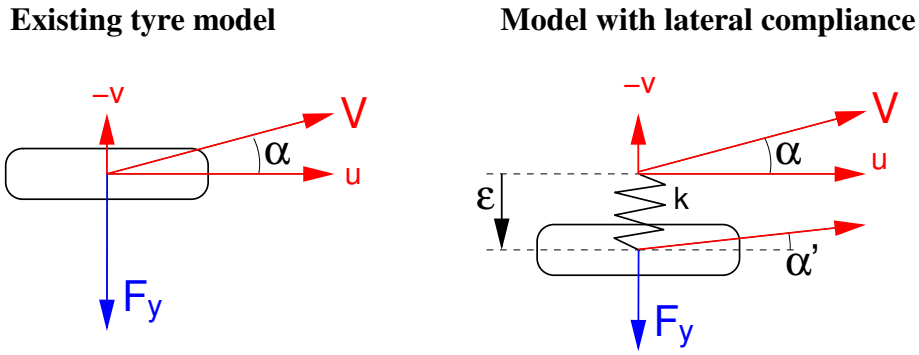

Figure 2.27. Existing and improved tyre model.

- existing tyre model:

$$F_y = C\alpha \tag{2.45}$$

with slip angle

$$\alpha = -\frac{v}{u} \tag{2.46}$$

- transient tyre model

$$F_y = C\alpha' = k\varepsilon \tag{2.47}$$

The transient slip angle is:

$$\alpha' = -\frac{v + \dot{\varepsilon}}{u} \tag{2.48}$$

Consequently we have with

$$C\dot{\alpha}' = k\dot{\varepsilon} \tag{2.49}$$

the first-order differential equation:

$$\frac{C}{k}\frac{1}{u}\dot{\alpha}' + \alpha' = -\frac{v}{u} = \alpha \tag{2.50}$$

Now, we will introduce the relaxation length σ:

$$\sigma = \frac{C}{k} \tag{2.51}$$

and

$$V \approx u \tag{2.52}$$

which lead to the final form of the differential equation:

$$\frac{\sigma}{V}\dot{\alpha}' + \alpha' = \alpha \tag{2.53}$$

We now have:

$$F_y = C\alpha' \tag{2.54}$$

For the first order response between lateral force and side slip angle input, the transfer function reads:

$$H_{F_y,\alpha}(s) = \frac{C}{\frac{\sigma}{V}s + 1} \tag{2.55}$$

The time constant is: σ/V.

The relaxation length σ does not depend on forward velocity V. Consequently:

- The response time reduces when the speed V increases.
- The travelled distance required to build up the lateral force remains the same

The response of F_y to a step change in α of 1 deg. has been shown in Figure 2.28. (C=1 kN/deg, σ=0.5 m)

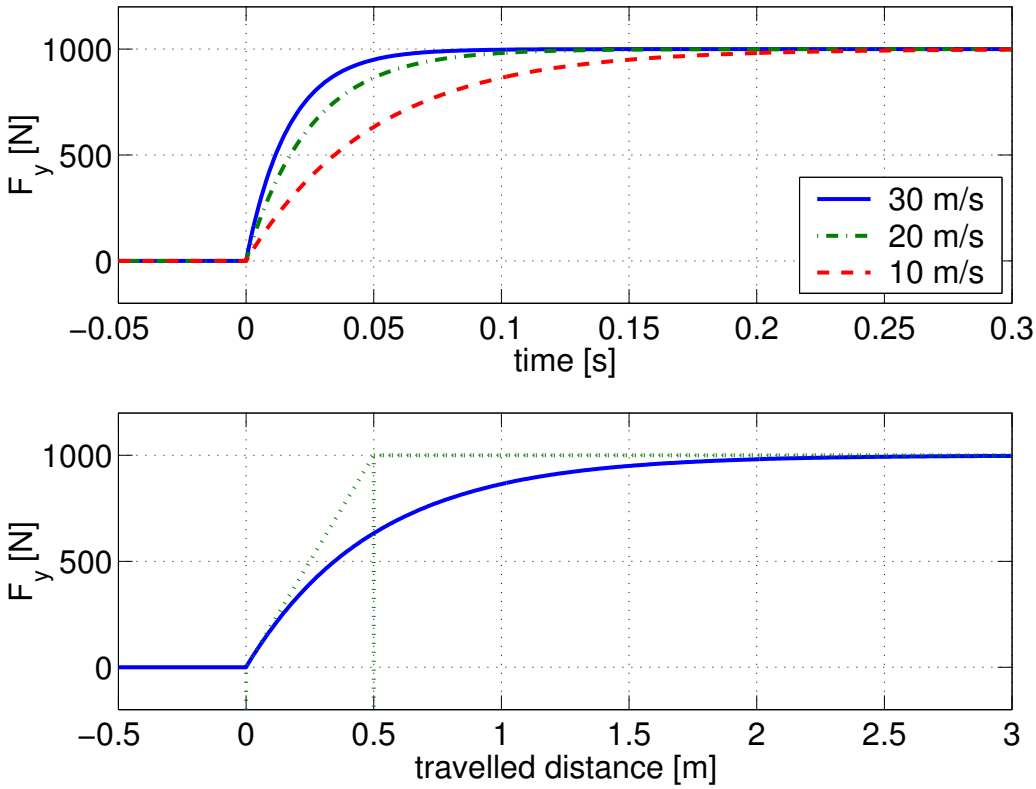

Figure 2.28. Step response at different speeds.

Tyre relaxation length measurement

The experiments have been carried out on the flat plank tyre tester.

- fixed steering angle (e.g. 1 deg.)
- velocity 0.05 m/s

Initially, the unloaded tyre is set at a steer angle (1 deg); then at t=0 the tyre is loaded and the rolling motion is commenced.

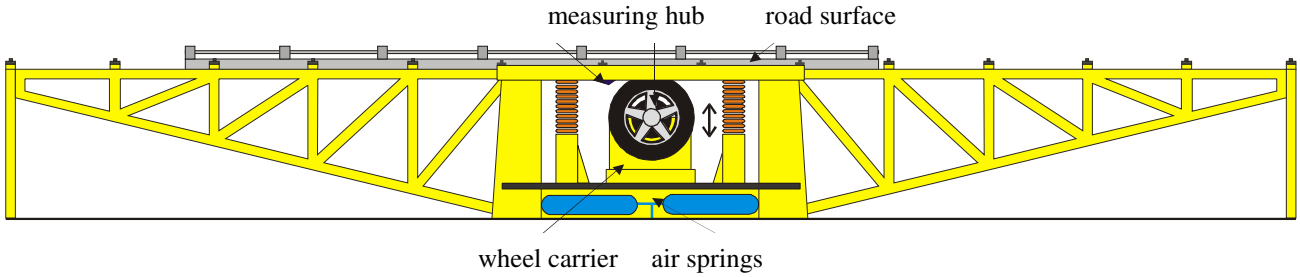

Figure 2.29. The flat plank machine for low speed tyre experiments.

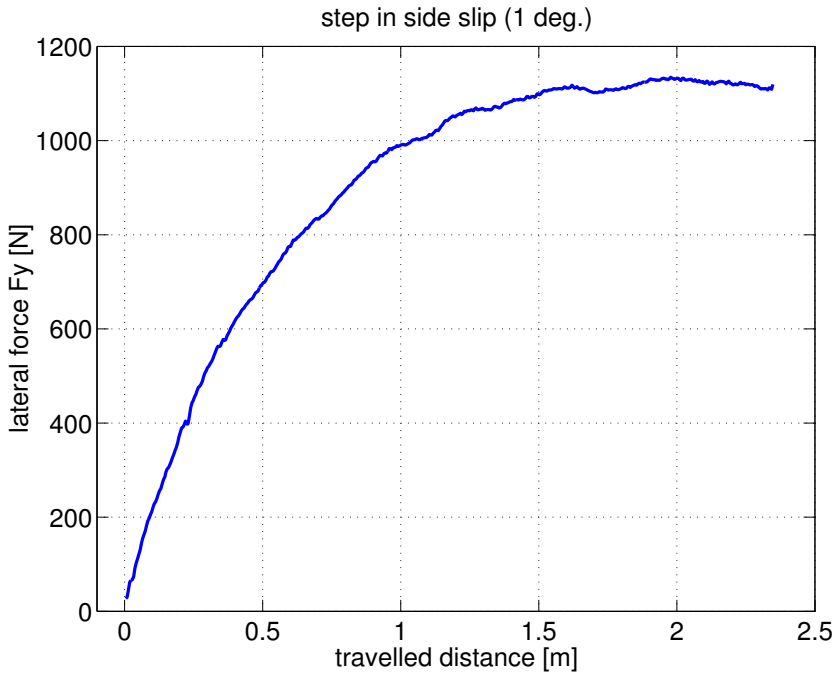

Figure 2.30. The measured response to a step change in slip angle.

Equations of motion of vehicle model including relaxation effects

We have (cf. Section 8.1 and FIGURE 8.1 of the book):

$$m(\dot{v} + ur) = C_1\alpha_1' + C_2\alpha_2' \tag{2.56}$$

$$I\dot{r} = aC_1\alpha_1' - bC_2\alpha_2' \tag{2.57}$$

$$\alpha_1 = \delta - \frac{1}{u}(v + ar) \tag{2.58}$$

$$\alpha_2 = -\frac{1}{u}(v - br) \tag{2.59}$$

$$\frac{\sigma}{u}\,\dot{\alpha}_1' + \alpha_1' = \alpha_1 \tag{2.60}$$

$$\frac{\sigma}{u}\,\dot{\alpha}_2' + \alpha_2' = \alpha_2 \tag{2.61}$$

with the following parameter values:

- m =1971.8 kg
- l = 2.88 m
- a =1.1907 m (based on vehicle weight distribution)
- $b = l - a$ = 1.6893 m
- I =3550 kgm^2
- C_1 =93000 N/rad (≈1600 N/deg)
- C_2 =137000 N/rad (≈2400 N/deg)
- σ_1 =0.57 m
- σ_2 =0.97 m
- i_s =17.0

2.1.6. Experimental validation

A random steer input has been applied in the vehicle test to achieve the frequency response functions.
Figures 2.31 and 2.32 present the frequency response functions for the lateral acceleration and the yaw rate to the input steer angle. We may compare the experimentally found results with those from model calculations.

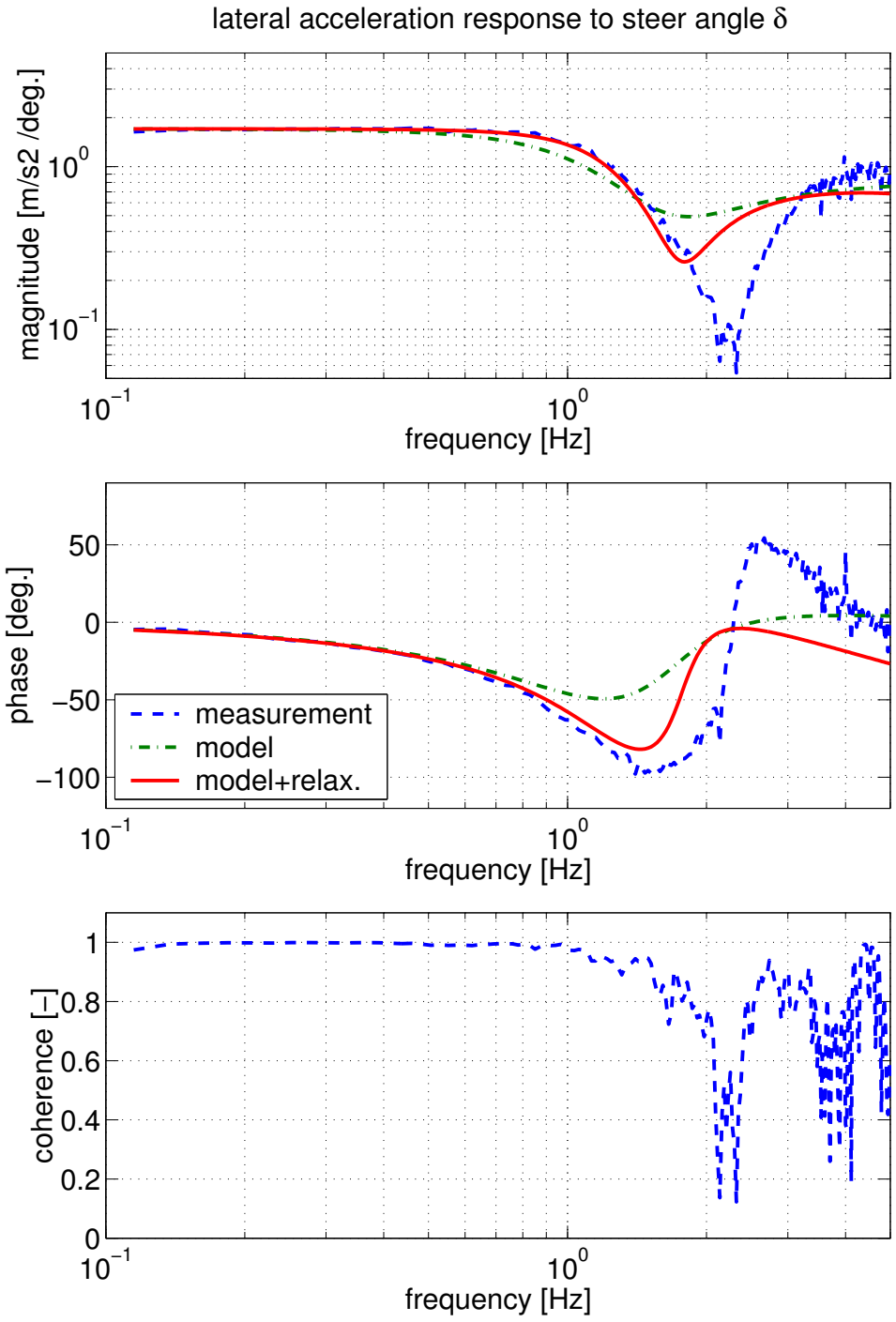

Figure 2.31. The frequency response function for the lateral acceleration.

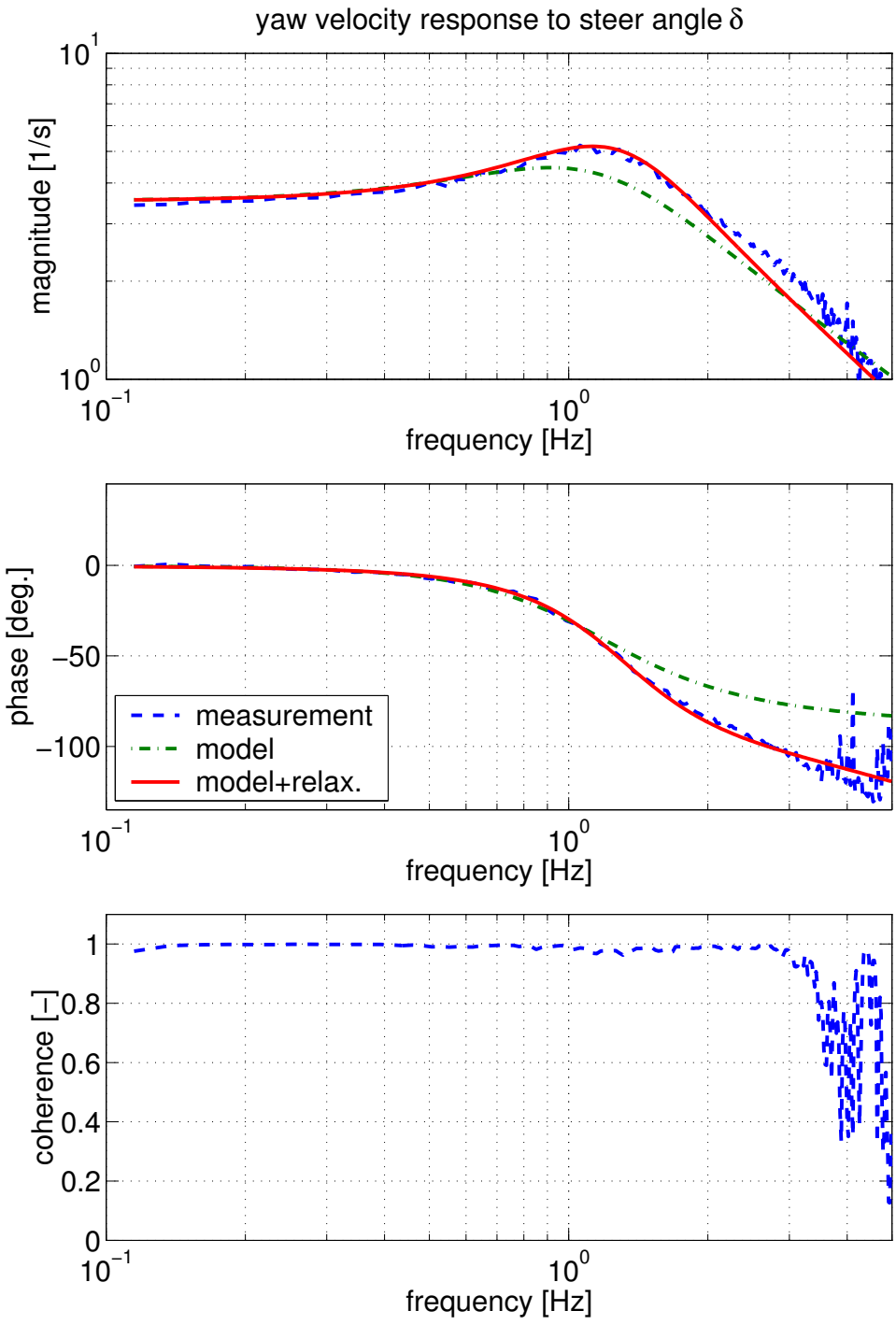

Figure 2.32. The frequency response function for the yaw velocity.

2.2. The non-linear system

We consider the steady-state cornering behaviour at large values of lateral acceleration a_y using the handling diagram (cf. Section 1.3.3 of the book).

2.2.1 The handling diagram

The following relations have been derived before (see Eqs. (2.21) and (2.22)):

$$\frac{l}{R} = \delta - (\alpha_1 - \alpha_2) \tag{2.62}$$

$$\alpha_1 - \alpha_2 = \frac{a_y}{g}\eta \tag{2.63}$$

so that

$$\alpha_1 - \alpha_2 = \frac{a_y}{g}\eta = \delta - \frac{l}{R} \tag{2.64}$$

We adopt the new graphical presentation (compare with Figure 2.5 that is 90 deg. rotated)

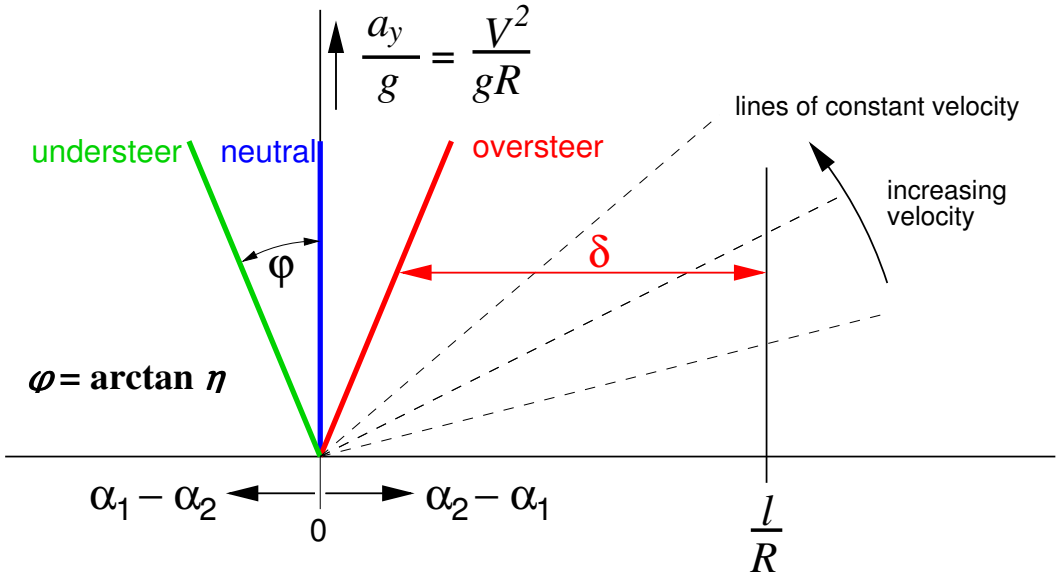

Figure 2.33. The handling diagram for the linear system.

Consider the equilibrium:

$$F_{y1} + F_{y2} = ma_y \qquad \text{(lateral)} \qquad (2.65)$$

$$F_{y1}a = F_{y2}b \qquad \text{(yaw)} \qquad (2.66)$$

$$F_{z1}a = F_{z2}b \qquad \text{(pitch)} \qquad (2.67)$$

Then

$$\frac{a_y}{g} = \frac{F_{y1} + F_{y2}}{mg} = \frac{F_{y1} + F_{y2}}{F_{z1} + F_{z2}} = \frac{F_{y1}}{F_{z1}} = \frac{F_{y2}}{F_{z2}} \qquad (2.68)$$

The lateral tyre force F_y is a non-linear function of the side slip angle α.

By subtracting the characteristics horizontally the handling diagram can be obtained!

The definition of oversteer/understeer is revised as follows:

- understeer if:

$$\frac{\partial \delta}{\partial V}\Big)_R > 0 \qquad (2.69)$$

- oversteer if:

$$\frac{\partial \delta}{\partial V}\Big)_R < 0 \qquad (2.70)$$

Note: We consider steady-state conditions. So in the test we need to have:

- very slow changes of V and δ.

In addition, we will carry out separate dynamic tests for validation.

- additional dynamic tests

2.2.2. Experimental validation

Estimate for normalised tyre characteristics

- linear part: already known
- non-linear part: chosen to get a good match with vehicle tests
- dotted part: not encountered during tests, educated guess…

The resulting diagrams presented below show good correspondence between theory (estimated characteristics) and experiment (considering the results of the linear model, Figures 2.21, 2.22 and 2.23).

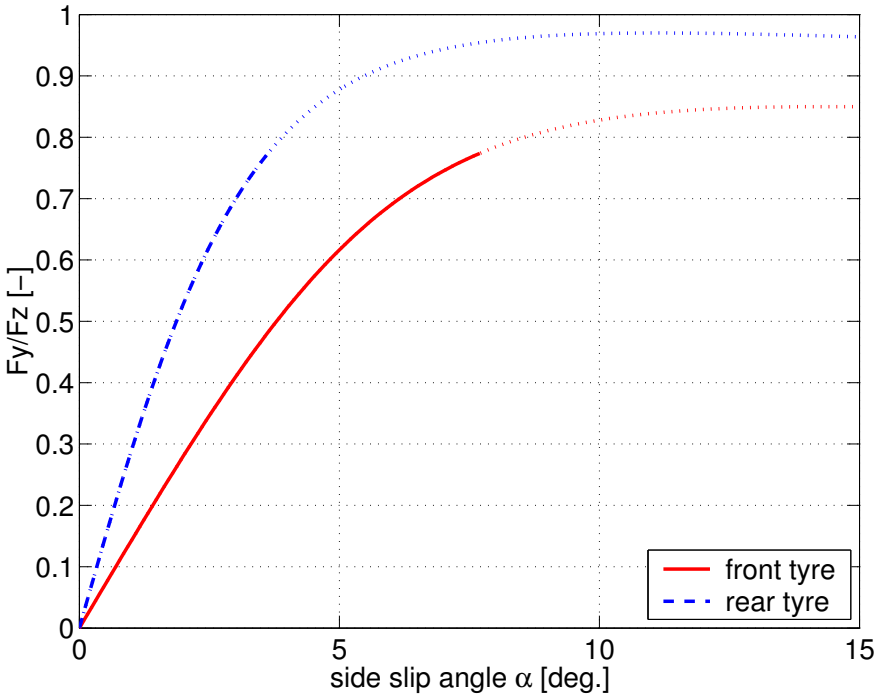

Figure 2.34. Estimated normalised tyre characteristics.

Note:
We have a simplified discussion: "tyre" includes compliance effects of the suspension design: although front and rear tyres may be same, the normalised front and rear tyre (or better: axle) characteristics will be different.

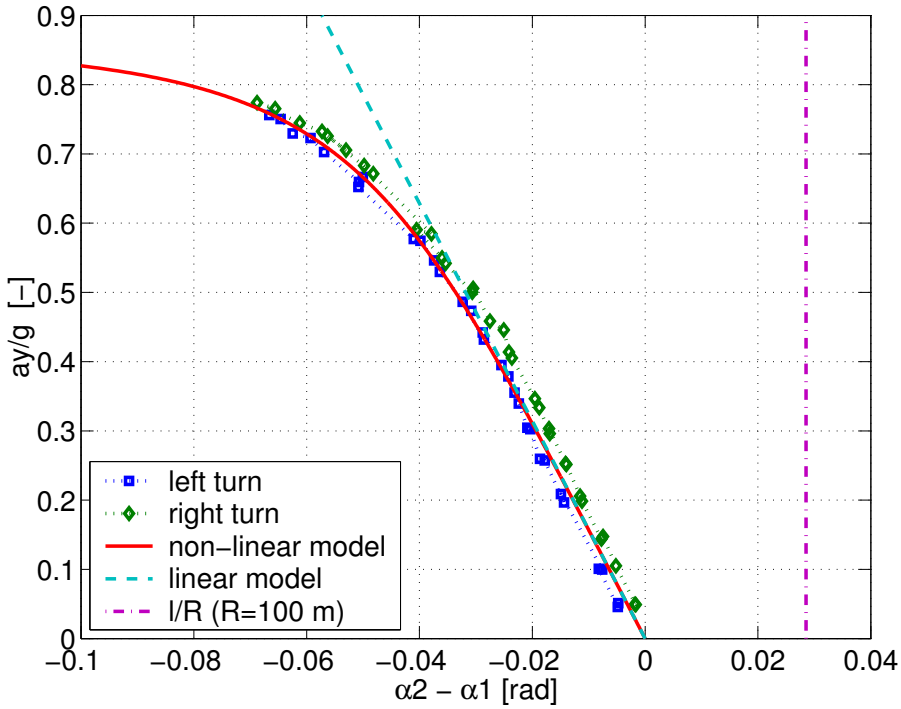

Figure 2.35. The resulting handling diagram.

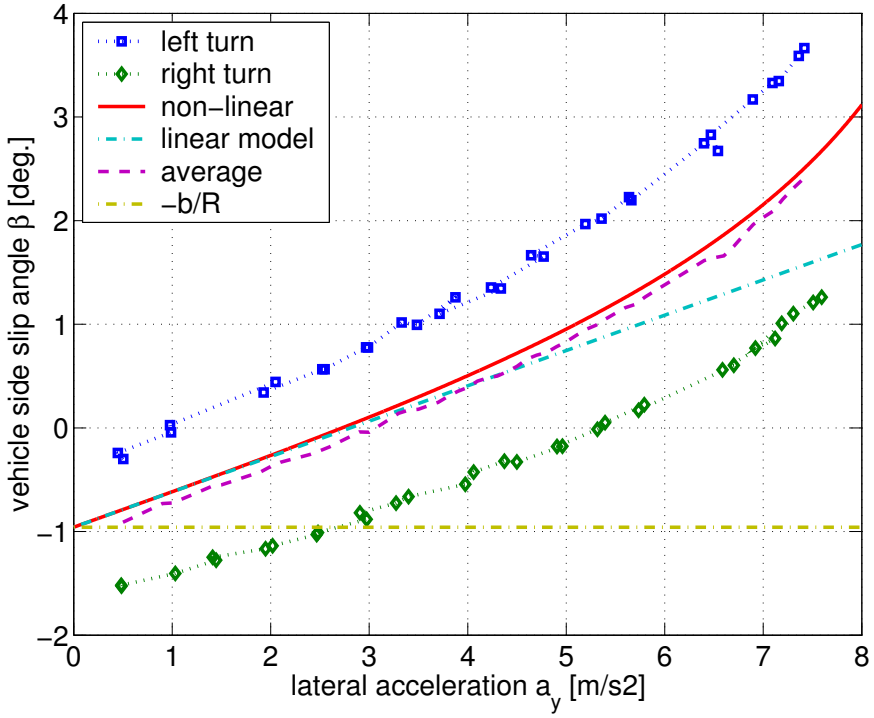

Figure 2.36. The vehicle slip angle β.

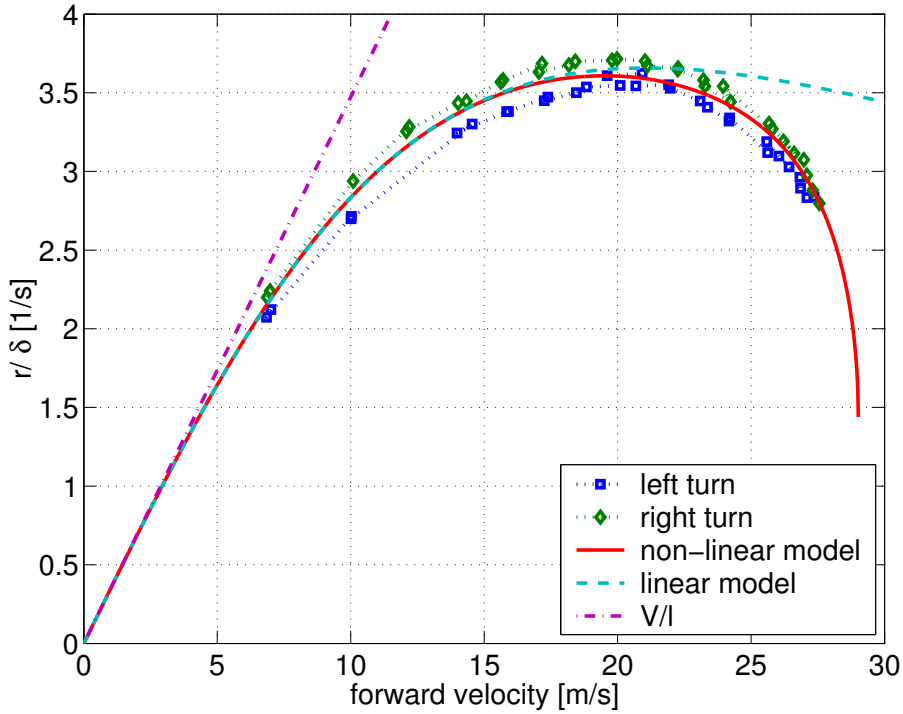

Figure 2.37. The yaw velocity gain.

Additional validation of the vehicle model through dynamic tests:

The following tests have been done:

- J-turn
- severe lane change

Lateral transient response performing a "J-turn"

- constant forward velocity (example 100 km/h)
- "step" steer input
- standardised in ISO 7401

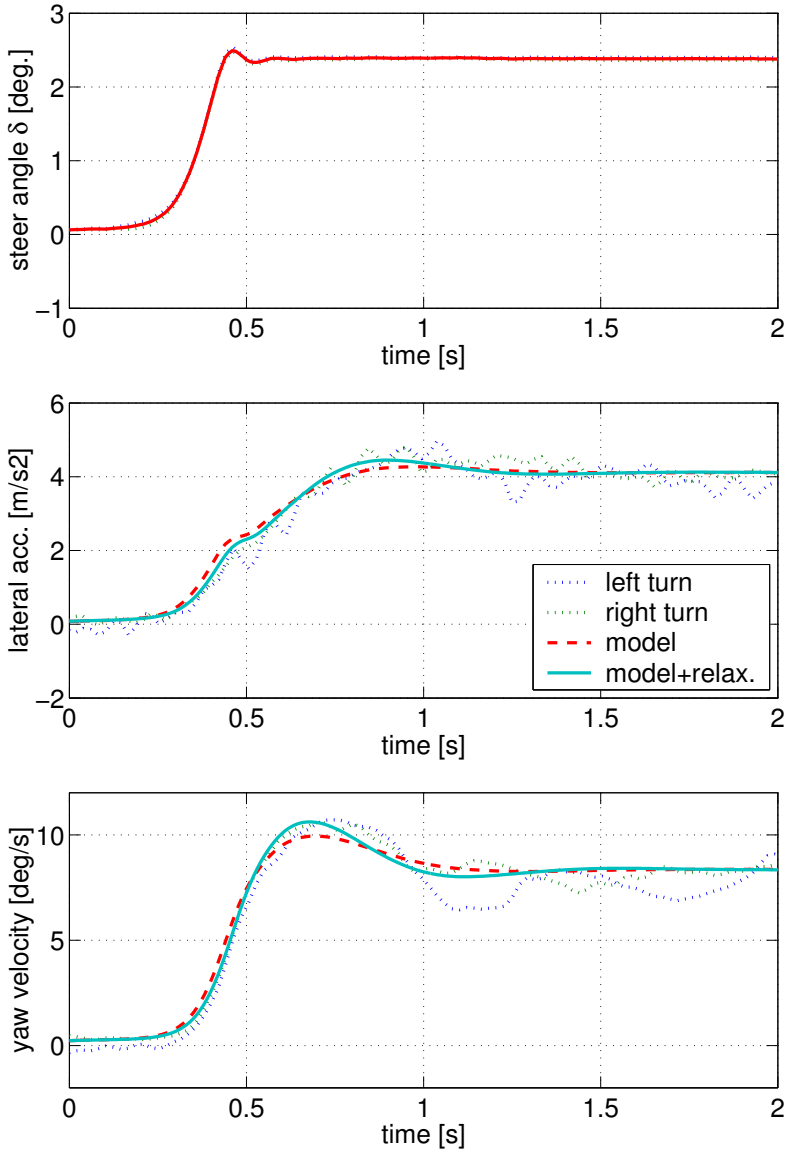

Figure 2.38. Vehicle response to a step change in steer angle (J-turn).

Severe lane change test

- obstacle avoidance
- find maximum velocity where test driver is capable to complete the course, without touching the cones
- high lateral accelerations, limit handling
- standardised in ISO/TR 3888

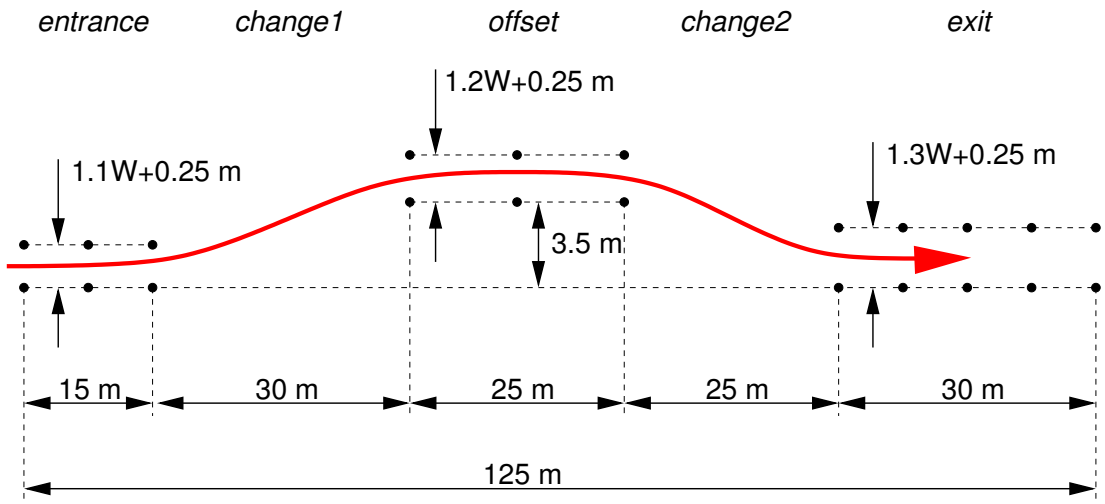

Figure 2.39. Lay-out for obstacle avoidance test. *w*: width of vehicle

simulation model:

- use measured steering angle and vehicle forward velocity as input
- model parameters from steady-state circular test and random steer (no additional tuning)
- compare against measurements:
  -linear model without relaxation effects
  -model with non-linear tyres and relaxation effects

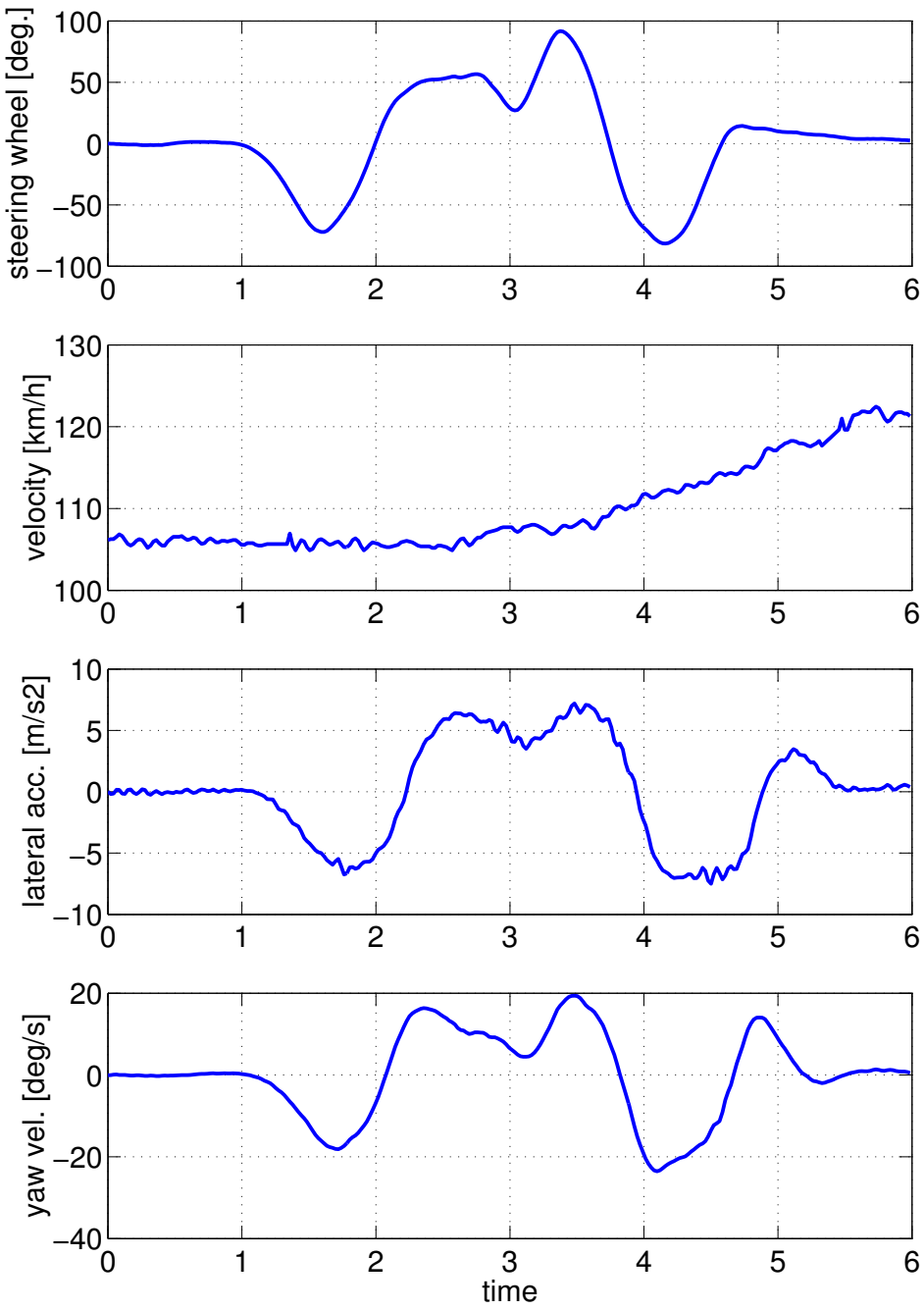

Figure 2.40. Measurement results of the obstacle avoidance test.

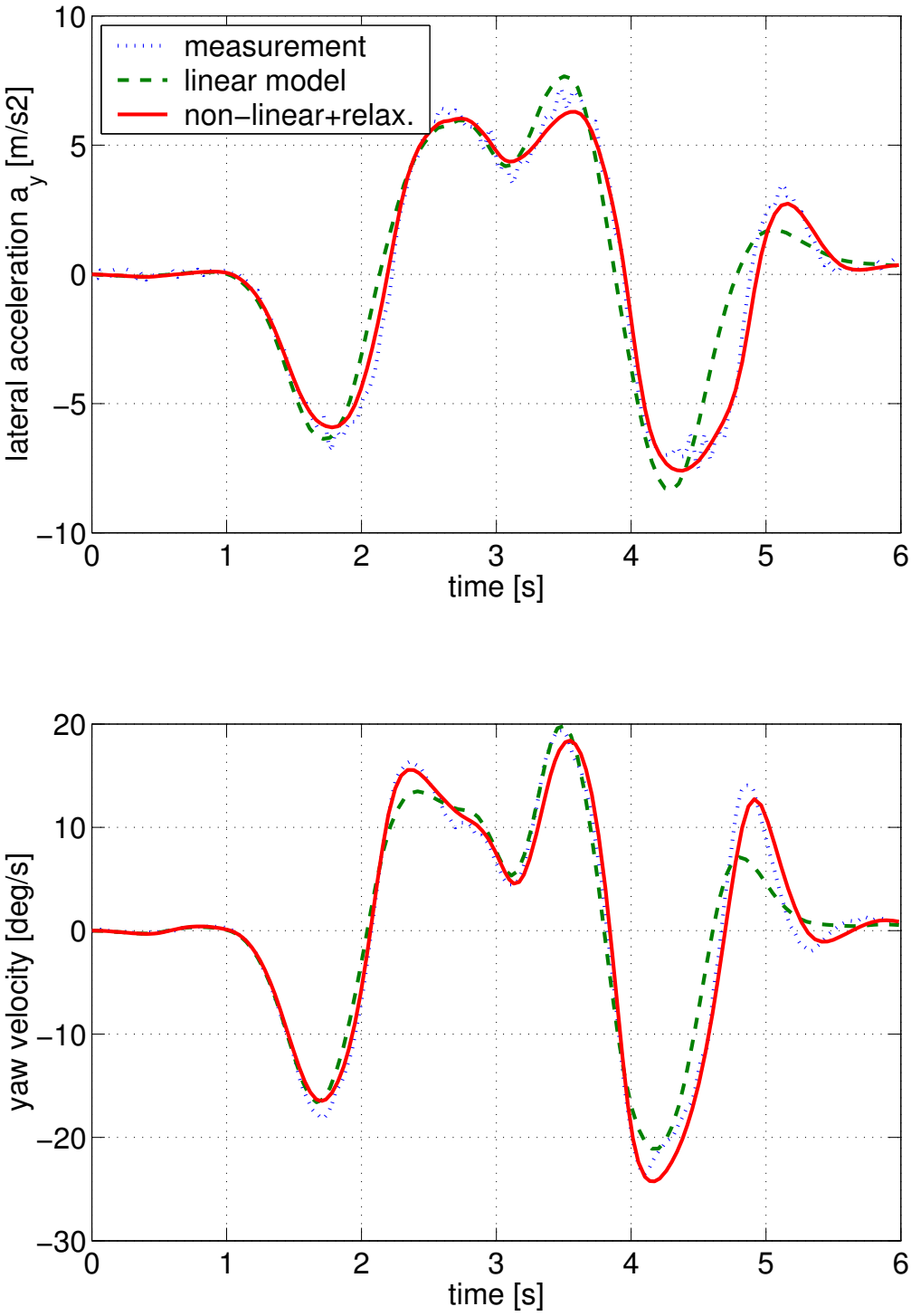

Figure 2.41. Comparison with different simulation models.